

Spatio-temporal variability of zooplankton standing stock in
eastern Arabian Sea inferred from ADCP backscatter
measurements

Ranjan Kumar Sahu, P. Amol, D.V. Desai, S.G. Aparna, D. Shankar

September 30, 2024

Abstract

We use acoustic Doppler current profiler (ADCP) backscatter measurements to map the spatio-temporal variation of zooplankton standing stock in the eastern Arabian Sea (EAS). The ADCP moorings were deployed at seven locations on the continental slope off the west coast of India; we use data from October 2017 to December 2023. The 153.3 kHz ADCP uses backscatter from sediments or organisms such as copepods, ctenophores, salps and amphipods greater than 1 cm to calculate current profile. The backscatter is obtained from echo intensity using RSSI conversion factor after doing necessary calibrations. The conversion from backscatter to biomass is based on volumetric zooplankton sampling at the respective locations. Analysis of the data over 24 – 120 m shows that the backscatter and zooplankton biomass decrease from the upper ocean (215 m g^{-3} biomass contour) to the lower depths. Changes are observed in the seasonal variation of the monthly

¹² climatology of zooplankton standing stock (integral of the biomass over 24 – 120 m water column)
¹³ as we move to poleward along the slope in EAS. The range of variation of standing stock is lowest
¹⁴ at Kanyakumari, followed by Okha, which lie at the southern and northern boundary of the EAS,
¹⁵ respectively. Complementary variables are used to explain the processes leading to growth or decay
¹⁶ of zooplankton biomass.

₁₇ **1 Introduction**

₁₈ **1.1 Background**

₁₉ Zooplankton plays a vital role in food web of pelagic ecosystem by enabling the hierarchical trans-
₂₀ port of organic matter from primary producers to higher trophic levels impacting the fish population
₂₁ and the carbon pump of the deep ocean [Ohman and Hirche, 2001, Le Qu et al., 2016]. They are
₂₂ presumably the largest migrating organisms in terms of biomass [Hays, 2003] which occurs in diel
₂₃ vertical migration (DVM). Zooplanktons depend not only on phytoplankton but other environ-
₂₄ mental parameters (e.g. Mixed layer depth, insolation, Oxygen, thermocline, nutrient availability,
₂₅ chlorophyll concentration and daily primary production). The biological productivity of the ocean
₂₆ is essentially connected with physics and chemistry [Subrahmanyam, 1959, Ryther et al., 1966,
₂₇ Qasim, 1977, Nair, 1970, Banse, 1995, McCreary et al., 2009, Vijith et al., 2016, Amol et al., 2020].
₂₈ The dynamic ocean results in varying physico-chemical properties, leading to bloom and growth of
₂₉ planktons in favourable conditions. The changes are strongly influenced by the seasonal cycle in the
₃₀ North Indian Ocean (NIO; north of 5 °N of Indian Ocean). The eastern boundary of Arabian Sea
₃₁ contains the West India Coastal Current (WICC; [Ramamirtham and Murty, 1965, Banse, 1968,
₃₂ McCreary Jr et al., 1993, Amol et al., 2014, Chaudhuri et al., 2020]) which reverses seasonally,
₃₃ flowing poleward (equatorward) during November to February (June to September).

₃₄ The direct consequence of this reversal is the seasonal cycle of thermocline, oxycline and thick-
₃₅ ness of mixed Layer Depth (MLD) induced by upwelling favourable conditions in summer and down-
₃₆ welling favourable conditions in winter in eastern Arabian Sea (EAS). Further, the phytoplankton
₃₇ biomass and chlorophyll concentration changes with the season [Subrahmanyam and Sarma, 1960,
₃₈ Banse, 1968, Lévy et al., 2007, Vijith et al., 2016]. Upwelling in summer monsoon leads to maximum

39 chlorophyll growth in the entire EAS [Banse, 1968, Banse and English, 2000, McCreary et al., 2009,
40 Hood et al., 2017, Shi and Wang, 2022]. During winter monsoon, the convective mixing induced
41 winter mixed layer [Shetye et al., 1992, Madhupratap et al., 1996b, Lévy et al., 2007, Vijith et al.,
42 2016, Shankar et al., 2016, Keerthi et al., 2017, Shi and Wang, 2022] results in winter chlorophyll
43 peak in northern EAS (NEAS) while the downwelling Rossby waves modulate chlorophyll along the
44 southern EAS (SEAS) albeit limited to coast and islands [Amol et al., 2020].

45 The zooplankton grazing peak is instantaneous with no time delay from peak phytoplankton
46 production [Li et al., 2000, Barber et al., 2001], but its population growth lags [Rehim and Imran,
47 2012, Almén and Tamelander, 2020] depending on its gestation period and other limiting aspects.

48 While some studies suggest that the peak timing of zooplankton may not change in parallel with
49 phytoplankton blooms [Winder and Schindler, 2004], others indicate that lag exists between primary
50 production and the transfer of energy to higher trophic levels [Brock and McClain, 1992, Brock et al.,
51 1991]. In their work, Aparna et al. [2022] (A22 from hereon) had shown non-linear interaction
52 between zooplankton and phytoplankton population. A22 showed that the zooplankton growth in
53 fact declines during upwelling facilitated increase in phytoplankton biomass. It implies the break
54 down of existing understanding of predator - prey relationship in fundamental level of marine food
55 chain with secondary production as a linear function of primary production.

56 The conventional zooplankton measurements, where only few snapshot/s of the event is captured
57 gives an incoherent or incomplete understanding in terms of spatio-temporal variation of zooplank-
58 ton [Ramamurthy, 1965, Piontkovski et al., 1995, Madhupratap et al., 1992, 1996a, Wishner et al.,
59 1998, Kidwai and Amjad, 2000, Barber et al., 2001, Khandagale et al., 2022] as much information
60 is revealed by later studies [Jyothibabu et al., 2010, Vijith et al., 2016, Shankar et al., 2019, Aparna
61 et al., 2022] using high resolution data. Calibrated acoustic instruments such as Acoustic Doppler

62 Current Profiler (ADCP) along with relevant data can be utilised to understand small scale vari-
63 ability [Nair et al., 1999, Edvardsen et al., 2003, Smith and Madhupratap, 2005, Smeti et al., 2015,
64 Kang et al., 2024], the complex interplay between the physico-chemical parameters and ecosystem
65 [Jiang et al., 2007, Potiris et al., 2018, Shankar et al., 2019, Aparna et al., 2022, Nie et al., 2023], the
66 zooplankton migration [Inoue et al., 2016, Ursella et al., 2018, 2021] and their seasonal to annual
67 variation [Jiang et al., 2007, Hobbs et al., 2021, Liu et al., 2022, Aparna et al., 2022].

68 The relationship between backscatter and the abundance and size of zooplankton was described
69 by Greenlaw [1979] wherein it was pointed out that single frequency backscatter can be used to esti-
70 mate abundance if mean zooplankton size is known. A drastic increase in study temporal and spatial
71 variation of zooplankton biomass using backscatter-proxy came in 1990s by introduction of high
72 frequency echo sounders, with studies [Flagg and Smith, 1989, Wiebe et al., 1990, Batchelder et al.,
73 Greene et al., 1998, Rippeth and Simpson, 1998] methodically showing acoustic backscatter
74 estimated zooplankton biomass. Net sampling augmented ADCP backscatter have been used to
75 study DVM and the spatial and temporal variability of zooplankton biomass in different marine
76 regions, such as the Southwestern Pacific, the Lazarev Sea in Antarctica and the Corsica Channel
77 in the north-western Mediterranean Sea [Cisewski et al., 2010, Hamilton et al., 2013, Smeti et al.,
78 2015, Guerra et al., 2019]. The first such study to exploit the potential of ADCPs in EAS was
79 carried out by A22 using ADCP moorings deployed on continental slopes off the Indian west coasts.

80 1.2 Objective and scope of the manuscript

81 A network of ADCPs has been installed off the continental slope and shelf on the west coast of
82 India. This ADCPs have enabled a rigorous view of intraseasonal to seasonal scale variability [Amol
83 et al., 2014, Chaudhuri et al., 2020] of WICC. In the recent study A22 have used ADCP moorings

84 off Mumbai, Goa and Kollam to explain the temporal variability of zooplankton biomass. The
85 study showed that the zooplankton peaks (and troughs) is not only non-uniform in latitude but
86 also heavily influenced by the oxygen minimum zone, MLD and the seasonal upwelling/downwelling
87 conditions. Stark contrast in the phytoplankton bloom and subsequence growth of zooplankton or
88 the lack thereof was observed in the EAS regimes.

89 We build upon the existing work by extending to include the newly incorporated ADCPs so as to
90 have a better understanding in the latitudinal variation of zooplankton biomass in EAS. The paper
91 is organized as follows; datasets and methods employed are described in detail in section 2. Section
92 3 describes the observed climatology of zooplankton biomass and standing stock. A comparison is
93 drawn to the results of A22. Further, the seasonal cycle of zooplankton biomass and standing stock
94 is discussed with relation to the MLD, oxygen, temperature and circulation in determining the
95 biomass is discussed in results section 4. Section 5 delves deeper into the intraseasonal variability
96 with summary and conclusion in section 6.

97 **2 Data and methods**

98 The backscatter data from ADCP and the zooplankton samples collected from the periphery of
99 mooring is described in this section. The backscatter derived from the echo intensity of the seven
100 ADCP mooring deployed on the continental slope off the Indian west coast is the primary data
101 we have use in this manuscript. The moorings details are summarized in [Table 1](#). In situ biomass
102 data from volumetric zooplankton samples are used to validate and correlate with backscatter. The
103 chlorophyll data is obtained from marine.copernicus.eu. In addition, we have used the monthly cli-
104 matology of temperature and salinity [[Chatterjee et al., 2012](#)] and the net primary productivity from
105 MODIS (Moderate Resolution Imaging Spectroradiometer) and VIIRS (Visible Infrared Imaging

¹⁰⁶ Radiometer Suite) from global NPP estimates (<http://sites.science.oregonstate.edu/ocean.productivity>).

¹⁰⁷ **2.1 ADCP data and Backscatter estimation**

¹⁰⁸ The ADCPs were deployed on the continental slope off the Indian west coast ([Fig. 1](#)), off Mumbai,
¹⁰⁹ Goa, Kollam and Kanyakumari, and later extended to three more sites to cover the entire EAS
¹¹⁰ basin from Okha (22.26°N) in north to Kanyakumari (6.96°N) in south. The other two ADCPs
¹¹¹ are Jaigarh at central EAS (CEAS) and Udupi in the transition zone between CEAS & SEAS. The
¹¹² extended moorings were deployed in October 2017, except for Kanyakumari which was deployed
¹¹³ earlier as well but it wasn't part of the earlier backscatter study by A22. The moorings are serviced
¹¹⁴ on yearly basis usually during October-November or in winter monsoon months. The ADCPs are
¹¹⁵ of RD Instruments make, upward-looking and operate at 153.3 kHz. While utmost care is taken to
¹¹⁶ position the instrument at ~ 200 m depth, yet for some deployments it's shallow or deeper owing
¹¹⁷ to drift caused by floater buoyancy-anchor weight balance. Data was collected at hourly interval
¹¹⁸ and the bin size was set to 4 m. The echoes at surface to 10 % range (~ 20 m) means the data at
¹¹⁹ these depths is rendered useless and is discarded from further use.

¹²⁰ We have followed the methodology laid down in A22 to derive the backscatter time series from
¹²¹ ADCP echo intensity data. The gaps up to two days are filled using the grafting method of
¹²² [Mukhopadhyay et al. \[2020\]](#) once the zooplankton biomass time series is constructed.

¹²³ **2.2 Zooplankton data and estimation of biomass**

¹²⁴ The zooplankton samples were collected in the vicinity (~ 10 km) of ADCP mooring site twice; once
¹²⁵ prior retrieval and again post deployment of moorings so that there is overlap in the ADCP time
¹²⁶ instance and in situ zooplankton samples. The sampling is done at the mooring location during

127 servicing cruises on board RV Sindhu Sankalp and RV Sindhu Sadhana ([table 2](#)). Multi-plankton
128 net (MPN) (100 μm mesh size, 0.5 m^2 mouth area) was used to get samples in the pre-determined
129 depth ranges; water volume filtered was calculated by the product of sampling depth range and the
130 mouth area of net. The depth range and timing of sample collection was different throughout the
131 MPN hauls (refer [Table 2](#)). From 2020 onward, the depth-range was standardized to the bins of 0
132 – 25, 25 – 50, 50 – 75, 75 – 100, 100 – 150 (units are in meters).

133 The backscatter obtained earlier is averaged in vertical corresponding to the specific MPN
134 hauls for each site. The backscatter is linear regressed with respective biomass to establish their
135 relationship, which has been demonstrated in numerous previous studies [[Flagg and Smith, 1989](#),
136 [Heywood et al., 1991](#), [Jiang et al., 2007](#), [Aparna et al., 2022](#)]. We calculated the regression equation
137 to be $y = 0.0203 x + 4.01$ and, which is well within the error range of the regression equation of
138 A22, $y = (0.02 \pm 0.004) x + (4.14 \pm 0.36)$ with a correlation of 0.53 ([Fig. 2](#)). The correlation value
139 in our case is 0.54; the minor difference is due to higher number of data points (159) in the present
140 study compared to A22 (67).

141 2.2.1 Biomass time series and estimation of standing stock

142 The zooplankton biomass time series ([Fig. 3](#)) is created from the above derived linear relationship:

143 $Bm = m * Sv + k$

144 where Bm is biomass taken in \log_{10} scale, m is slope, Sv denotes backscattering strength and k
145 is the intercept. The standing stock is determined by taking the depth integral of biomass over the
146 water column. To maintain the consistency of standing stock estimation, only those deployments
147 that doesn't lack data at any depth in the entire range of 24 – 120 m are considered for analysis
148 as in A22. The lack of data in the above mentioned depth range is due to deviation in positioning

149 of ADCP sensor in the water column. A swift alteration in bathymetry along the continental slope
150 implies that the mooring might anchor at a different depth than planned, hence a change in the
151 predicted position of ADCP. This leads to gap in data at few mooring sites for some year. For
152 example, for the northern-most mooring at Okha, data is not available for the entire upper 120
153 m depth for the second deployment. Also at Jaigarh, where the surface to ~60m data (in 3rd
154 deployment) and Kollam, where 80 m and below (in 4th deployment) is unavailable and hence
155 discarded from standing stock estimation. There are few deployments where no data or bad data
156 was recorded e.g, at Udupi (4th deployment) and Kanyakumari (6th deployment).

157 **2.3 Mixed-layer depth, temperature and oxygen**

158 As we are using a 153.3 kHz ADCP moored at ~ 150 m, the top ~ 10% of data is unusable because
159 of surface echoes. MLD in EAS is of the order ~ 20 to 40 m during summer monsoon [Shetye
160 et al., 1990, Sreenivas et al., 2008] especially in the SEAS, but during winter the MLD in northern
161 NEAS remains deep [Shankar et al., 2016]. Although it is possible to use the near-surface ADCP
162 data after due noise correction; it is beyond the scope of present study. The temperature data is
163 used from Chatterjee et al. [2012], a monthly climatology having 1 ° spatial resolution. Monthly
164 climatology of oxygen data is obtained from World Ocean Atlas 2013 [García et al., 2014] which
165 contains objectively analyzed 1 ° climatological fields of in situ measurements.

166 **2.4 Chlorophyll and net primary productivity data**

167 Previous study based on ADCP data of EAS A22 have used SeaWiFS based chlorophyll data for
168 comparison with climatology of zooplankton standing stock (ZSS). The SeaWiFS was at its end
169 of service in 2010, hence we use new chlorophyll product. While the chlorophyll product only

¹⁷⁰ captures chlorophyll at surface, the productivity models consists information in depth containing
¹⁷¹ the subsurface chlorophyll maxima. The present study has been conducted using Global Ocean
¹⁷² Colour, biogeochemical, L3 data obtained from the [E.U. Copernicus Marine Service Information](#).
¹⁷³ The daily data is available at a spatial resolution of 4 km.

¹⁷⁴ 3 Climatology of zooplankton biomass and standing stock

¹⁷⁵ The high biomass regime in the upper ocean and low biomass regime in deeper depths is differen-
¹⁷⁶ tiated using a biomass contour: 215 mg m^{-3} off Mumbai, Goa, Kollam, Jaigarh and Udupi,
¹⁷⁷ $mg m^{-3}$ off Okha and Kanyakumari. For simplicity, this biomass contour is abbreviated to be z215
¹⁷⁸ & z175 and its depth is denoted as D215 & D175, respectively. The choice of biomass contour isn't
¹⁷⁹ abrupt; first, it is carefully chosen to accommodate the seasonal variation, as a shift to biomass
¹⁸⁰ contour lower than the z215 would be unviable as our data is only till 140 m depth, for example in
¹⁸¹ the case of Kollam, the D215 exceeds 140 during few months of 2022 ([Fig. 3](#)). A higher biomass
¹⁸² contour would lead to inferior view of the seasonal cycle as in the case of Kanyakumari and Okha
¹⁸³ where 215 mg m^{-3} biomass contour is often low enough to reach $\sim 20 - 30$ m depths, hence z175 is
¹⁸⁴ chosen here. Second, it allows us to link the seasonal variation of biomass to the physico-chemical
¹⁸⁵ properties. Climatology of zooplankton biomass and ZSS is discussed at locations northward start-
¹⁸⁶ ing from southernmost mooring site i.e, Kanyakumari. The time series is discussed briefly in the
¹⁸⁷ following section.

¹⁸⁸ The previous study of zooplankton by A22 in EAS based on ADCP backscatter was consisting
¹⁸⁹ of three sites: Mumbai in NEAS, Goa in CEAS and Kollam in SEAS from 2012 to 2020. The
¹⁹⁰ extended mooring sites are at Okha at NEAS, Jaigarh at CEAS, Udupi in the transition zone of
¹⁹¹ CEAS & SEAS and Kanyakumari at SEAS is the southern most location in our study area. The

¹⁹² monthly climatology of biomass and ZSS is computed for all locations having valid data in 24 – 140
¹⁹³ m depth range ([Fig. 4](#)). A comparison is made in later paragraphs with availability of new data.

¹⁹⁴ 3.1 Southern EAS

¹⁹⁵ During mid-March off Kanyakumari, the depth of 23 ° C isotherm (henceforth D23) shallows along-
¹⁹⁶ with oxycline (marked by 2.1 ml L^{-1}) and a rise in biomass is observed ([Fig. 4 g1](#)). The z175 is
¹⁹⁷ shallower from May onward to October and the zooplankton biomass is comparatively higher than
¹⁹⁸ rest of the year. D175 deepens starting from October and the relatively high biomass in water
¹⁹⁹ column is maintained till late December. However, the deepening of D175 isn't reflected as an
²⁰⁰ increase in ZSS because of low biomass in the entire water column. A gradual increase is seen in
²⁰¹ the chlorophyll biomass starting from April and the peak is attained in June ([Fig. 4 g2](#)). The ZSS
²⁰² is increased in June, however the growth is minimal. There is almost no seasonal variation in ZSS
²⁰³ off Kanyakumari (ZSS std, 0.67 gm m^{-2}) as compared to the ZSS variation at the nearest northern
²⁰⁴ mooring site off Kollam (ZSS std, 1.25 gm m^{-2}), where a strong seasonal cycle is observed and the
²⁰⁵ D215 is deeper for any given month.

²⁰⁶ Off Kollam, a higher biomass is present in the larger portion of water column and the D215
²⁰⁷ is at ~ 110 m during Mar-May ([Fig. 4 f1](#)). Starting from March, the D215 begins to shallow
²⁰⁸ with progress in time till August. During this period, a sharp decrease is seen in the D23 (\sim
²⁰⁹ 80 m in June to September) while the oxycline (1.7 ml L^{-1}) overshoots the thermocline ([Fig. 4](#)
²¹⁰ f1). A steep rise in chlorophyll biomass is seen off Kollam and its peak is attained in August
²¹¹ ([Fig. 4 f2](#)). The ZSS declines in the same period and reaches a minimum when the chlorophyll
²¹² biomass is at its peak. The chlorophyll biomass decreases rapidly in the following months, while
²¹³ the ZSS increases and a maximum is seen during October. This feature was earlier reported by A22

214 showing disproportionate interaction between zooplankton and phytoplankton. A similar feature
215 is seen further north, off Udupi which sits at the transition zone of SEAS & CEAS, albeit with
216 a relatively weaker zooplankton biomass. The peak of chlorophyll and minimum of ZSS occurs in
217 September ([Fig. 4 e2](#)) which is one month later than off Kollam. The 2.1 ml L^{-1} oxygen contour
218 overshoots thermocline, however it reaches to a much shallow depth of $\sim 20 \text{ m}$ during July to
219 October unlike any other location in our EAS study area. The D215 vaguely follows D23; with
220 the gradual shallowing from March onward reaching $\sim 60 \text{ m}$ in September and a steep decline
221 afterwards till November ([Fig. 4 e1](#)).

222 3.2 Central EAS

223 Off Goa, the D215 seasonal trend is similar to Udupi and is entirely restricted by D23 & 1.7 ml L^{-1}
224 oxygen contour that closely follows it. Although we witness an increase in chlorophyll biomass
225 in October, the D215 is restricted to the $\sim 50 \text{ m}$ in this period and the ZSS is at its minimum
226 similar to off Udupi (Kollam) during September (August). The ZSS rapidly increases and reaches
227 its maximum in January, sustained till March and then gradually declines. Unlike the previous
228 locations, the biomass off Goa decreases rapidly below the z215 as reported earlier in A22, reaching
229 as low as 60 mg m^{-3} at 130 m during June to September ([Fig. 4 d1](#)).

230 The ZSS off Jaigarh is identical but stronger to that of off Goa, owing to an higher biomass
231 above z215 and the comparatively deeper D215 ([Fig. 4 c1](#)). From the ZSS maximum in February
232 ([Fig. 4 c2](#)), it steadily decreases and attains a minimum in September, a rapid rise is seen in the
233 following months. What's intriguing is a presence of strong seasonal cycle in ZSS off Jaigarh (std
234 3.24 gm m^{-2} , highest among all locations) although the seasonal variation in chlorophyll biomass
235 ([Fig. 4 c2](#)) is visibly non-existent (0.05 mg m^{-3} Chl std, lowest among all locations). This is an

236 exact opposite scenario of Kanyakumari, where an insignificant seasonal variation in ZSS (0.67
237 $gm\ m^{-2}$ ZSS std) is seen even though the chlorophyll biomass varies strongly ($0.51\ mg\ m^{-3}$ Chl
238 std).

239 Starting from Kollam (Fig. 4 f1) and moving northward to Jaigarh (Fig. 4 c1), we see that the
240 core of high zooplankton biomass gradually shifts from summer (off Kollam) to winter monsoon (off
241 Jaigarh), with the transition of upper ocean zooplankton biomass happening along Udupi and Goa.
242 On the contrary, the chlorophyll biomass tends to have low seasonal range as we move northward
243 from SEAS, with Jaigarh having the least seasonal variation.

244 3.3 Northern EAS

245 Further north off Mumbai the D215 is deeper in December to early April, resulting in a higher
246 ZSS (Fig. 4 b2). D23 follows D215 and the oxycline follows an erratic pattern, reaching depths
247 > 140 during January to March (Fig. 4 b1); when a higher biomass is observed above z215. The
248 chlorophyll biomass shows seasonal variation albeit lower than the SEAS counterpart. The ZSS
249 increases rapidly from its minima in October in the following month as the D215 deepens and
250 the maximum occurs in February. The chlorophyll biomass decreases from March and a gradual
251 decrease in ZSS is seen till July, after which the ZSS basically flattens even though the chlorophyll
252 increases.

253 At the northernmost site of EAS i.e, off Okha, a noticeable feature is a much higher oxygen
254 in upper ocean except during summer monsoon. The biomass above z175 is much weaker (Fig. 4
255 a1) leading to a relatively lower ZSS (Fig. 4 a2) compared to Mumbai. The D175 shallows from
256 February to it's minimum in August. There's two chlorophyll peak off Okha; one in February due
257 to convective mixing induced deepening of MLD [Keerthi et al., 2017] and the other during August

258 in summer monsoon [Lévy et al., 2007]. The ZSS remains flat in summer monsoon period i.e, June
259 to September, although the chlorophyll biomass increases in this time. Afterwards, ZSS gradually
260 increases and attains its maximum in February same as the chlorophyll biomass. ZSS sustains this
261 maximum till March, declines rapidly in April and then gradually till July.

262 **3.4 Comparison to biomass and ZSS climatology of A22**

263 It is observed that D215 is shallower at all locations and as a result a lower biomass and ZSS as
264 seen in the climatology of the present study ([Fig. 5](#)). The difference in D215 is prominent off Goa;
265 while in the previous climatology ([Fig. 5 b1](#)) the D215 is deeper and lies along D23, in the present
266 climatological data the D215 is shallower and lies $\sim 20 - 40$ m above the D23 during January to
267 April ([Fig. 5 b2](#)). A relatively lower biomass is present above z215 year round which reflects in
268 overall lower ZSS of Goa and Mumbai. In the present data, the ZSS maxima off Mumbai occurs in
269 March instead of February (A22), due to a lower ZSS value. The second maxima occurs in August
270 ([Fig. 5 d1](#)) and is less pronounced in recent data ([Fig. 5 d2](#)). There is dramatic decrease in the
271 minima off Mumbai that occurs in October and ZSS increases rapidly afterwards till February. Off
272 Kollam, higher biomass occurs from May to June in A22, and from May to June and September to
273 November in the present study, with a ZSS minima in August ([Fig. 4 c2, d2](#)). The higher ZSS on
274 either side to this minima is less pronounced in A22. This difference in ZSS is clearly seen in the
275 correlation, which is 0.60 off Kollam, while it is 0.94 and 0.98 off Mumbai and Goa, respectively. The
276 correlation reflects ZSS trend similarity, not magnitude deviation over time. In the present study,
277 chlorophyll biomass peaks across all locations in August, revealing a zooplankton-phytoplankton
278 relationship discrepancy off Kollam, consistent with A22 findings.

²⁷⁹ **3.5 Time series of zooplankton biomass**

²⁸⁰ A preliminary analysis of the biomass time series in daily and monthly averaged scale shows that
²⁸¹ the biomass decreases with increasing depth ([Fig. 3](#)) at all the seven locations. Rate of biomass
²⁸² decrease with depth, roughly defined as the difference between mean biomass at 40 m and 104 m
²⁸³ depth is highest off Jaigarh and Mumbai as it has higher biomass in upper ocean ([Fig. 6 c,b](#)) and
²⁸⁴ lowest off Kanyakumari. This is followed by CEAS locations Goa and Udupi ([Fig. 6 d,e](#)). While the
²⁸⁵ biomass decrease with depth is lower off Kollam from 2017 to 2020, it becomes considerably high
²⁸⁶ from thereon ([Fig. 6 f](#)). A pattern that develops with lower mean biomass off Okha (northernmost
²⁸⁷ of EAS) and off Goa (CEAS) bifurcated by higher mean biomass off Mumbai & Jaigarh; while the
²⁸⁸ lower mean biomass off Udupi (CEAS) and off Kanyakumari (Southernmost of EAS) is divided by
²⁸⁹ higher mean biomass off Kollam. From standard deviation of biomass it is inferred that the sites
²⁹⁰ with higher biomass tends to have higher variation over time as in the case of Mumbai, Jaigarh and
²⁹¹ Kollam. The mean, standard deviation of biomass, ZSS and chlorophyll are shown in [Table 3](#). A
²⁹² comparatively weaker decline in zooplankton biomass with respect to depth off Okha ([Fig. 3 a1,a2](#))
²⁹³ at NEAS is agreeing with earlier reported data [[Wishner et al., 1998](#), ?, [Smith and Madhupratap,](#)
²⁹⁴ [2005](#), [Jyothibabu et al., 2010](#)] where oxygen deficit is thought to be the cause, particularly during
²⁹⁵ summer monsoon seen in [García et al. \[2014\]](#) climatology (figure not shown). The sites at SEAS,
²⁹⁶ especially off Kanyakumari and 2017 to 2020 off Kollam also have weaker decrease [[Madhupratap](#)
²⁹⁷ [et al., 2001](#), [Jyothibabu et al., 2010](#), [Aparna et al., 2022](#)]. However, post 2020 the decline in
²⁹⁸ biomass with depth off Kollam is high owing to a strong bloom in these years reflected as deepening
²⁹⁹ of D215. While the z175 and z215 is deeper in winter monsoon throughout EAS, upper ocean shows
³⁰⁰ considerably high biomass during this period at NEAS. On the contrary at SEAS, the upper ocean
³⁰¹ shows higher biomass during summer monsoon even though the D215 & 175 is shallower in this

302 period.

303 4 Seasonal cycle and variability

304 This section will deal with a discussion on the seasonal cycle and variability of biomass and ZSS in
305 annual and intra-annual scale along the three regimes of EAS.

306 The time series data is incomplete due to instrument issues or incorrect ADCP placement. For
307 example, Okha's second deployment (2019-2020) lacked data for the top 140 meters because the
308 instrument was too deep. This makes it hard to analyze annual cycles in regions with limited data.
309 Therefore, we consider locations other than Okha and Jaigarh for the 40-meter biomass in annual
310 scale. The ZSS time series is obtained by integrating the biomass over 24 – 120 m of water column,
311 ([Fig. 9](#)). The biomass is decomposed into distinct period bands spanning days to months. Among
312 these, DVM is the simplest variation, determining zooplankton biomass at a given depth with
313 higher(lower) biomass at night(day). The strength and contribution of components of variability
314 changes over time and differs between EAS regimes. For instance, in 2019 off Kollam, short-term
315 variability was dominated by high-frequency components as found by beta value of Fourier analysis.
316 An increase in biomass during the summer monsoon was due to low-frequency variabilities. How-
317 ever, a sharp decline in August resulted from decreasing intra-annual and intra-seasonal variability,
318 despite weakly positive annual variability. More new information can be unearthed if variability at
319 each time scale is studied further.

320 From the linear equation correlating biomass and backscatter, the upper and lower bound of
321 error limits equals to $\sim 14 \text{ mg m}^{-3}$. The standard deviation incorporating 99.73 % data i.e, $\pm 3 *$
322 σ of intraseasonal variability is $\pm 40 \text{ mg m}^{-3}$ resulting in its range of 80 mg m^{-3} . The intra-annual
323 (annual) variability also has a range of 80 mg m^{-3} (35 mg m^{-3}). This higher range of variability

324 compared to the error range permits us to infer information reliably.

325 4.1 SEAS

326 The annual cycle of biomass off Kanyakumari (Udupi & Kollam) is weak (strong), but it varies
327 in time. The absence of ZSS annual cycle off Kanyakumari is confirmed with wavelet analysis
328 ([Fig. 9 g1](#)). Off Kollam, the wavelet power is stronger post 2020 ([Fig. 7 f](#)) and the presence of an
329 weak annual cycle in ZSS is seen contrary to a strong annual cycle of Udupi. A biennial peak is
330 observed in Fourier analysis of ZSS of Kollam agreeing with A22. Along with the annual cycle, we
331 observe presence of semi-annual (~ 180 days) cycle at most locations and together they constitute
332 the seasonal cycle. It is observed that the semi-annual cycle is comparable or stronger than the
333 annual cycle at some instances such as off Kollam (2018 & 2022) and Udupi (2018). Both annual
334 and semi-annual cycles weakens with depth at SEAS sites.

335 To capture the annual variability, the biomass is filtered with lanczos filter within period of 300
336 to 400 days. The variability declines strongly with depth off Kollam, although such feature is absent
337 at remaining two SEAS sites. The annual variability off Kanyakumari (22 mg/m^{-3}) is least among
338 all mooring sites, although Kollam and Udupi show strong annual variability. The variability at
339 intra-annual (100 – 250 days) band tends to be stronger compared to the annual variability and
340 is strengthened during late summer monsoon to transitional monsoon months ([Fig. 13](#)) as seen
341 during 2021 (off Udupi) and 2021,2022 (off Kollam). Fourier analysis of the daily biomass time
342 series suggests presence of signals within the intra-annual band off Kanyakumari, e.g, power peaks
343 at ~ 140 and ~ 220 days implying that the variability is strictly restricted to narrow bands within
344 intra-annual band.

345 **4.2 CEAS**

346 Annual cycle of biomass is comparatively weak off Goa (CEAS) contrary to results of A22 which
347 could be due to shorter time record and low biomass in the recent years as reflected in its ZSS for
348 2018 to early 2020 ([Fig. 9 d1](#)). At Goa and Jaigarh, we see that the semi-annual period dominates
349 seasonal cycle in the same duration ([Fig. 7 d](#)). The dominance of semi-annual cycle is also seen
350 off Kollam. Although the dominance of semi-annual period in seasonal cycle is seen only for some
351 years, a similar feature was discussed for WICC where the intra-annual component dominates the
352 seasonal cycle as we go equatorward with a change in the strength of intra-annual component
353 in time [[Chaudhuri et al., 2020](#)]. The higher intra-annual variability often coincides with shallow
354 D215/D175, for example off Goa during 2020 and 2022, and weak variability coincides with constant
355 depth of D215. This transient nature of variability is due to the spread of energy among all intra-
356 annual periods for 2022 ([Fig. 7](#)) off Goa, while during 2020 the wavelet energy is only present in
357 the semi-annual periods, resulting in a overall weaker intra-annual component.

358 Upward phase propagation in filtered zonal and meridional currents is noted at most mooring
359 sites [[Amol et al., 2014](#)] and in the annual filtered biomass ([Fig. 12](#)) off Goa and southern moorings,
360 we shed a light on this in discussion section using wavelet coherence result.

361 **4.3 NEAS**

362 Off Mumbai, a strong annual cycle (~ 365 days) dominates the seasonal cycle throughout the time
363 series of biomass (40 m ([Fig. 7](#)) & 104 m [Fig. 8](#)) and ZSS ([Fig. 9](#)). The semi-annual cycle is present
364 at 40 m ([Fig. 7](#)) off Mumbai but weakens at 104 m([Fig. 8](#)) resulting in a annual cycle dominated
365 ZSS. Analysis reveals the presence of strong semi-annual cycle off Okha (at 104 m only).

366 The annual variability is strong off Mumbai and Jaigarh (at CEAS & NEAS transition zone)

367 with 3σ range of 41 and 54 mg m^{-3} , respectively, which is highest among EAS regimes. As observed
368 in ocean currents [Amol et al., 2014, Chaudhuri et al., 2020], the annual filtered biomass decreases
369 moderately with depth off Mumbai and the three CEAS sites than off Kollam (Fig. 11). Intra-annual
370 variability of biomass decreases poleward (excluding Kanyakumari) with higher variation seen off
371 Kollam, Udupi and Goa. Off Okha the annual (intra-annual) variability is weaker (comparable) to
372 the variability off Mumbai but with a weak seasonal cycle at upper ocean.

373 5 Intraseasonal variability

374 The intraseasonal band, defined as the variability occurring between periods of few days to 90 days
375 is split into two categories; a high-frequency (period < 30 days) and a low-frequency ($30 <$ period
376 < 90 days) component. The presence of significant variation in the 30-day running mean with
377 recurring bursts are seen in the daily data and in the wavelet analysis of biomass at 40 m (Fig. 7)
378 and 104 m (Fig. 8) as bursts during few months distinctive to each mooring location.

379 The wavelet power at 40 m in low-frequency intraseasonal band peaks during September to
380 December off Mumbai, Jaigarh and Kanyakumari while no such general observation is found in
381 other locations. However, the wavelet power at 104 m in comparison to 40 m suggests a decrease in
382 its strength at respective locations. Lanczos filtered biomass in 30 to 90 day period shows that the
383 intraseasonal variability is strong during August to November off all location (Fig. 14). This is in
384 contrast to the WICC intraseasonal band which is strong during winter monsoon [Amol et al., 2014,
385 Chaudhuri et al., 2020]. The low frequency intraseasonal variability is higher in the upper ocean,
386 however it can extend to deeper depths (~ 140) for some years e.g., off Kollam during 2022 (Fig. 14
387 f). The magnitude of low-frequency intraseasonal component is high as we move equatorward till
388 Kollam and declines off Kanyakumari (Fig. 14 g). As noted earlier in variability of the intra-

389 annual component, the intra-seasonal component is transient and its magnitude is higher than the
390 low frequency variabilities. A strong dependency of zooplankton biomass on the intra-seasonal
391 variation has implication on the sampling of zooplankton.

392 It is to be noted that while the annual cycle dominates the WICC [Amol et al., 2014, Chaudhuri
393 et al., 2020, 2021], contrary to this, the intra-seasonal variability that dominates the zooplankton
394 biomass along EAS. On the other hand, the direction of WICC at any given time of the year
395 is unpredictable [Chaudhuri et al., 2020] and advection & entrainment can affect zooplankton
396 biomass, we can expect it to produce such behaviors that can only be resolved with high-frequency
397 intraseasonal variations. Strong peaks in intraseasonal band in chlorophyll was evident in Fourier
398 analysis, similar to zooplankton biomass and ZSS, but lacked concrete evidence of direct correlation.

399 6 Discussion

400 6.1 Summary

401 The zooplankton biomass and standing stock across different regions of EAS was examined in this
402 article, highlighting their spatio-temporal trends in the light of physico-chemical parameters using
403 the multi-yearlong ADCP backscatter data from 2017 to 2023.

404 The findings shows notable seasonal variation in zooplankton biomass and ZSS; In SEAS the
405 higher biomass is observed during summer monsoon, while in NEAS the high biomass is observed
406 during winter monsoon with transition of peak biomass happening gradually along CEAS regime
407 (Fig. 4). Off Kollam, a unique double peak in ZSS occurs, one during May to July and another
408 in September to November, suggesting a complex interplay between environmental drivers and
409 zooplankton growth (Fig. 4 f2). Off Kanyakumari, the seasonal variation in ZSS is non-existent

410 even though a dramatic seasonality is seen in primary production. Climatology shows strong decline
411 in biomass w.r.t. depth off Goa, then NEAS sites off Jaigarh, Mumbai and Okha followed by SEAS
412 locations off Udupi, Kollam and Kanyakumari.

413 Seasonal cycle play a crucial role in regulating biomass variability. A strong annual cycle is
414 observed in Northern sites like Mumbai and Jaigarh ([Figs. 7 and 8](#)), with biomass peaking during
415 winter monsoon months ([Fig. 4](#)). However, the Southern and Central regions, particularly off
416 Kollam, exhibit more complex patterns. Off Kollam, the presence of a weak annual cycle and a
417 stronger semi-annual cycle is noted along with a moderately strong biennial cycle. The semi-annual
418 cycle is especially prominent in the Southern EAS, where it contributes significantly to the seasonal
419 biomass changes, while Northern regions is dominated by annual cycle.

420 Intraseasonal variability, particularly in the 30 - 90 day range, is found to influence zooplankton
421 biomass significantly, especially in the summer monsoon months ([Fig. 14](#)), while the high frequency
422 (period $< \sim 30$ days) variability determine changes in smaller temporal scale ([Fig. 10](#)). Intraseasonal
423 variability is higher in the Southern EAS, with the Northern regions displaying more stable patterns.
424 The variability in annual scale is weak, while that in intra-annual scale is often comparable to
425 intraseasonal variability. The dependence of biomass on the current is investigated showing linkage
426 in the annual scale as seen off Goa at near-surface depths.

427 6.2 Physico-chemical drivers of zooplankton biomass

428 Numerous factors have an impact on the zooplankton population dynamics and growth in the
429 EAS. Throughout the summer monsoon, the Somali current, which flows clockwise in Arabian sea,
430 is essential in moving oxygen-depleted waters creating a perennial oxygen minimum zone (OMZ)
431 [[Sarma et al., 2020](#), [Sudheesh et al., 2022](#)]. The net transport of water in upper 500 m of northern

432 Arabian sea is about 5 Sv and a majority of the replaced waters comes from upwelling in the eastern
433 Arabian sea [Shi et al., 1999] during summer monsoon with the high-nutrient water covering \sim 500-
434 700 km from coast [Morrison et al., 1998]. Upwelling supplies nutrients to the surface [Kumar et al.,
435 2000], but it also plays a role in the creation of hypoxic conditions, which can restrict the kinds of
436 zooplankton species that can survive in these waters [Jayakumar et al., 2004]. The upwelling starts
437 in early by February itself off SEAS, but it occurs much later during May farther north along the
438 coast [Banse, 1968, Kumar et al., 2000, Vijith et al., 2016, Sarma et al., 2020] albeit weaker than
439 the southern counterpart. The deepening of MLD in winter due to convective mixing during [Marra
440 and Barber, 2005, Shankar et al., 2016, Shi and Wang, 2022] leads to dilution of zooplankton grazers
441 in water column [Marra and Barber, 2005] and hence longer food chain [Banse, 1995, Barber et al.,
442 2001], explaining the carnivore dominated fisheries in NEAS [Shankar et al., 2019] and planktivore
443 dominated SEAS [Longhurst and Wooster, 1990, Shankar et al., 2019].

444 The southwest monsoon was found to be the most productive period [Kumar et al., 2000]
445 however the observed primary productivity values were lower than predicted primary productivity
446 owing to efficient grazing by mesozooplankton that kept diatom biomass in check instead of high
447 levels of primary productivity as seen in coastal upwelling regions [Barber et al., 2001]. Similar
448 to the zooplankton variability, the inter-annual variability of Chl-a is less in comparison to its
449 seasonal variability [Shi and Wang, 2022] implying the inter-species relationship to be at play in
450 shorter timescale with large and small phytoplankton dominating the SEAS [Shankar et al., 2019].
451 It is inferred that along with the physico-chemical parameters, the biology of ocean determines
452 the zooplankton-phytoplankton relationship and their biomass, respectively. This interdependency
453 of planktons and the physico-chemical drivers shows up as strong intra-seasonal and intra-annual
454 variability in zooplankton biomass as demonstrated in section 4.

455 **6.3 Current and biomass coherence**

456 The annual variability shows that the contribution of this band to the time series of total biomass is
457 very weak. It is low off Kanyakumari (standard deviation 3.64 mg m^{-3}) and Okha (3.73 mg m^{-3}),
458 while it is stronger at rest of the basin, with strongest variability off Jaigarh (9.05 mg m^{-3}). But
459 the variation in chlorophyll biomass off Jaigarh is much lower than that of Kanyakumari. Owing
460 to the above and coherence of current and ZSS, advection as a driver to upwelling and further as
461 one of the cause for zooplankton growth is hypothesized and their relationship is explored. Wavelet
462 coherence shows that the current and biomass have strong coherence off Kanyakumari (2019,2021),
463 Kollam (2019, 2022) during May to late summer monsoon of 2019 with meridional current leading
464 biomass, when the currents are reversing with monsoon (Fig. 12). As we go poleward along the
465 slope, coherence exists but at different depth i.e, off Goa for 2019, the maximum coherence of
466 meridional current with biomass is at 50 to 80 m and again below 110 m. The feature observed
467 in annual filtered biomass off Goa is similar to the alongshore component [Nethery and Shankar,
468 2007], with the core of biomass and alongshore current lying at about 50 m. Further north, off
469 Mumbai a shift in time of maximum coherence is observed occurring in winter monsoon at 80 m
470 and below with zonal current leading biomass. During pre-summer monsoon upwelling sets as early
471 as February in SEAS but only in May farther north along the coast [Banse, 1968] which results
472 in shift in biomass coherence as we go poleward. Off Okha however, present of coherence is seen
473 throughout 2021 from 20 to 150 m with meridional current leading biomass which could be due
474 to a deeper MLD in northern NEAS [Marra and Barber, 2005, Shankar et al., 2016]. This has
475 implications on the nature of zooplankton and fisheries found in regimes of EAS as we'll discuss in
476 the following section.

477 **6.4 Decoding the Arabian sea paradox: evolution of our understanding**

478 A servicing cruise along the EAS moorings takes about 12 to 15 days excluding the time to and fro
479 from port to first/last mooring [Chaudhuri et al., 2020, Aparna et al., 2022]. However, a sampling
480 cruise dedicated to study the spatial variation of zooplankton [Madhupratap et al., 1992, Smith
481 et al., 1998, Wishner et al., 1998, Kidwai and Amjad, 2000], say for summer monsoon may last a
482 month or more with coarse sampling interval and hence fail to capture the actual biomass within a
483 season for a fair spatial comparison. One such occasion is a dip in zooplankton biomass off Kollam
484 because of intra-seasonal variability during August, 2019 (Fig. 10). The resulting biomass is low
485 even though the primary production in SEAS [Asha Devi et al., 2010, Jyothibabu et al., 2010] is
486 high and subsequent zooplankton biomass is supposed to be high.

487 While the zooplankton biomass was expected to have a seasonality, the transient nature of
488 variability also explains why Arabian sea paradox was seen as such. In northern Arabian sea,
489 the extended upwelling time leads to a longer and steady primary production, albeit weaker than
490 the southern counterpart [Madhupratap et al., 1996a, Smith and Madhupratap, 2005]. Provided
491 the zooplankton-phytoplankton interaction is based on primary production, this may lead to the
492 zooplankton biomass to be consistent over season or longer i.e, weaker intraseasonal and intra-
493 annual variability, for example off Goa, June 2019 to September 2020, (Figs. 13 and 14) the D215
494 remains at same depth, and this could be misinterpreted as constancy in zooplankton biomass
495 leading to paradoxical conclusions.

496 Using the continuous data from ADCP backscatter, A22 showed not only there is a seasonality,
497 but zooplankton-phytoplankton relationship can interact unexpectedly by negative zooplankton
498 growth (dip in ZSS) when the phytoplankton bloom occurs during summer monsoon as was the
499 case of Kollam. However, with the present study extending further boundary of EAS in south

500 of Kollam, we come across Kanyakumari which matches with the paradox posited back in 1990s
501 by [Madhupratap et al. \[1992, 1996a\]](#), [Smith and Madhupratap \[2005\]](#) and studies from JGOFS
502 cruise. Although the difference between the former and present paradox is fundamentally distinct,
503 while former raised the question "how does zooplankton sustain it's population/growth in unviable
504 conditions throughout year?", the present question is "why zooplankton doesn't seem to grow
505 in tune with raising phytoplankton productivity during summer monsoon?". The answer to this
506 question may lie in understanding the intricate interactions between phytoplankton, zooplankton,
507 and fish, as well as the influence of monsoon currents on the availability of essential nutrients and
508 rare elements that zooplankton need but cannot obtain from phytoplankton alone. [[Shankar et al.,](#)
509 [2019](#)] had found that if the upwelling is sufficiently strong, then phytoplankton tend to grow bigger
510 in size and hence fish can compete directly with zooplankton on predation of phytoplankton, thereby
511 limiting the zooplankton growth substantially which we see as a minuscule rise in ZSS ([Fig. 4 g2](#)).
512 For similar reasoning, a dip in ZSS is observed in peak summer monsoon off Kollam during August.

513 6.5 Conclusion

514 The results presented in this paper are based on the ADCP backscatter which is suitable for
515 creating long-term time series of zooplankton biomass in open ocean. There are however, certain
516 limitations to this approach. While the variation in depth is captured with in situ samples from
517 MPN, the variation in season is not adequately addressed owing to the limitation of months when
518 ADCP servicing cruises are undertaken. The west coast cruises for ADCP servicing are planned
519 for the monsoon transition months but may start as early as late September till December with
520 few exceptions such as 2022 when it was carried out in March. Since the intraseasonal and intra-
521 annual variability is almost double that of the annual one, the sampling done in particular season

522 for biomass-backscatter comparison isn't sufficient. For a better approach to capture the seasonal
523 variation, more in situ samples are needed from the less explored seasons.

524 While we are able to infer the biomass information, any information regarding the size distribu-
525 tion of zooplankton and their contribution to ZSS is lost. In western Arabian sea, microzooplank-
526 ton dominated the grazing processes by consuming approximately 71 % of the primary production
527 [Reckermann and Veldhuis, 1997, Marra and Barber, 2005, Landry, 2009]. Mesozooplankton, in
528 turn relied on microzooplankton for about 40 % of their food [Landry, 2009, Hood et al., 2024].
529 However, the relative grazing importance of micro and mesozooplankton fluctuated seasonally and
530 spatially, affecting the overall impact on phytoplankton biomass in a way that aligns with the
531 theory of grazing control or trophic cascade [Ripple et al., 2016] in the Arabian Sea [Marra and
532 Barber, 2005, Landry, 2009]. To understand the intricate complexities of meso and microzooplank-
533 ton interaction and their size distribution, multi-frequency, size-resolving backscatter data can be
534 utilised.

535 **7 Declaration of competing interest**

536 The authors declare that they have no known competing financial interests or personal relationships
537 that could have appeared to influence the work reported in this paper.

538 **8 Acknowledgments**

539 The data were collected by xxx with fund provided under xxxx. The mooring programme is
540 supported by INCOIS (Indian National Centre for Ocean Information Services, Hyderabad) and
541 CSIR. We acknowledge the contribution of mooring division and ship cell of CSIR-NIO.

542 Ranjan Kumar Sahu expresses his acknowledgment to the Council of Scientific and Industrial
543 Research (CSIR) for sponsoring his fellowship. Additionally, he extends his thanks to Ashok
544 Kankonkar for providing the essential data, Rahul Khedekar for his data processing, Roshan D'Souza
545 for his diligent work in biological data analysis. Their contributions were invaluable to the successful
546 completion of this research.

547 References

- 548 Anna-Karin Almén and Tobias Tamelander. Temperature-related timing of the spring bloom and match between
549 phytoplankton and zooplankton. *Marine Biology Research*, 16(8-9):674–682, 2020.
- 550 P Amol, D Shankar, V Fernando, A Mukherjee, SG Aparna, R Fernandes, GS Michael, ST Khalap, NP Satelkar,
551 Y Agarvadekar, et al. Observed intraseasonal and seasonal variability of the west india coastal current on the
552 continental slope. *Journal of Earth System Science*, 123(5):1045–1074, 2014.
- 553 P Amol, Suchandan Bemal, D Shankar, V Jain, V Thushara, V Vijith, and PN Vinayachandran. Modulation of
554 chlorophyll concentration by downwelling rossby waves during the winter monsoon in the southeastern arabian
555 sea. *Progress in Oceanography*, 186:102365, 2020.
- 556 SG Aparna, DV Desai, D Shankar, AC Anil, Shrikant Dora, and R Khedekar. Seasonal cycle of zooplankton standing
557 stock inferred from adcp backscatter measurements in the eastern arabian sea. *Progress in Oceanography*, 203:
558 102766, 2022.
- 559 C.R. Asha Devi, R. Jyothibabu, P. Sabu, Josia Jacob, H. Habeebrehman, M.P. Prabhakaran, K.J. Jayalakshmi, and
560 C.T. Achuthankutty. Seasonal variations and trophic ecology of microzooplankton in the southeastern arabian
561 sea. *Continental Shelf Research*, 30(9):1070–1084, 2010. ISSN 0278-4343. doi: <https://doi.org/10.1016/j.csr.2010.02.007>. URL <https://www.sciencedirect.com/science/article/pii/S0278434310000439>.
- 563 Carin J Ashjian, Sharon L Smith, Charles N Flagg, and Nasseer Idrisi. Distribution, annual cycle, and vertical
564 migration of acoustically derived biomass in the arabian sea during 1994–1995. *Deep Sea Research Part II:*
565 *Topical Studies in Oceanography*, 49(12):2377–2402, 2002.
- 566 K Banse and DC English. Geographical differences in seasonality of czcs-derived phytoplankton pigment in the
567 arabian sea for 1978–1986. *Deep Sea Research Part II: Topical Studies in Oceanography*, 47(7-8):1623–1677, 2000.
- 568 Karl Banse. Hydrography of the arabian sea shelf of india and pakistan and effects on demersal fishes. In *Deep sea*
569 *research and oceanographic Abstracts*, volume 15, pages 45–79. Elsevier, 1968.
- 570 Karl Banse. Zooplankton: pivotal role in the control of ocean production: I. biomass and production. *ICES Journal*
571 *of marine Science*, 52(3-4):265–277, 1995.

- 572 Richard T Barber, John Marra, Robert C Bidigare, Louis A Codispoti, David Halpern, Zackary Johnson, Mikel
573 Latasa, Ralf Goericke, and Sharon L Smith. Primary productivity and its regulation in the arabian sea during
574 1995. *Deep Sea Res. Part 2 Top. Stud. Oceanogr.*, 48(6-7):1127–1172, jan 2001.
- 575 WE Barraclough, RJ LeBrasseur, and OD Kennedy. Shallow scattering layer in the subarctic pacific ocean: detection
576 by high-frequency echo sounder. *Science*, 166(3905):611–613, 1969.
- 577 H. P. Batchelder, J. R. VanKeuren, R. D. Vaillancourt, and E. Swift. Spatial and temporal distributions of acoustically
578 estimated zooplankton biomass near the marine light-mixed layers station (59°30'n, 21°00'w) in the north atlantic
579 in may 1991. *Journal of Geophysical Research: Oceans*, 100:6549–6563, 1995. doi: 10.1029/94jc00981.
- 580 John C Brock and Charles R McClain. Interannual variability in phytoplankton blooms observed in the northwestern
581 arabian sea during the southwest monsoon. *Journal of Geophysical Research: Oceans*, 97(C1):733–750, 1992.
- 582 John C Brock, Charles R McClain, Mark E Luther, and William W Hay. The phytoplankton bloom in the north-
583 western arabian sea during the southwest monsoon of 1979. *Journal of Geophysical Research: Oceans*, 96(C11):
584 20623–20642, 1991.
- 585 Abhisek Chatterjee, D Shankar, SSC Shenoi, GV Reddy, GS Michael, M Ravichandran, VV Gopalkrishna,
586 EP Rama Rao, TVS Udaya Bhaskar, and VN Sanjeevan. A new atlas of temperature and salinity for the north
587 indian ocean. *Journal of Earth System Science*, 121:559–593, 2012.
- 588 Anya Chaudhuri, D Shankar, SG Aparna, P Amol, V Fernando, A Kankonkar, GS Michael, NP Satelkar, ST Khalap,
589 AP Tari, et al. Observed variability of the west india coastal current on the continental slope from 2009–2018.
590 *Journal of Earth System Science*, 129(1):57, 2020.
- 591 Anya Chaudhuri, P Amol, D Shankar, S Mukhopadhyay, SG Aparna, V Fernando, and A Kankonkar. Observed
592 variability of the west india coastal current on the continental shelf from 2010–2017. *Journal of Earth System
593 Science*, 130:1–21, 2021.
- 594 Boris Cisewski, Volker H Strass, Monika Rhein, and Sören Krägesky. Seasonal variation of diel vertical migration
595 of zooplankton from adcp backscatter time series data in the lazarev sea, antarctica. *Deep Sea Research Part I:
596 Oceanographic Research Papers*, 57(1):78–94, 2010.
- 597 Kent L Deines. Backscatter estimation using broadband acoustic doppler current profilers. In *Proceedings of the
598 IEEE Sixth Working Conference on Current Measurement (Cat. No. 99CH36331)*, pages 249–253. IEEE, 1999.
- 599 A Edvardsen, D Slagstad, KS Tande, and P Jaccard. Assessing zooplankton advection in the barents sea using
600 underway measurements and modelling. *Fisheries Oceanography*, 12(2):61–74, 2003.
- 601 S Fielding, G Griffiths, and HSJ Roe. The biological validation of adcp acoustic backscatter through direct comparison
602 with net samples and model predictions based on acoustic-scattering models. *ICES Journal of Marine Science*,
603 61(2):184–200, 2004.

- 604 Charles N Flagg and Sharon L Smith. On the use of the acoustic doppler current profiler to measure zooplankton
605 abundance. *Deep Sea Research Part A. Oceanographic Research Papers*, 36(3):455–474, 1989.
- 606 H. E. García, R. A. Locarnini, T. P. Boyer, J. I. Antonov, A. V. Mishonov, O. K. Baranova, M. M. Zweng, J. R.
607 Reagan, and D. R. Johnson. Dissolved oxygen, apparent oxygen utilization, and oxygen saturation. *NOAA Atlas*
608 *NESDIS 75*, 3, 2014.
- 609 Charles H Greene, Peter H Wiebe, Chris Pelkie, Mark C Benfield, and Jacqueline M Popp. Three-dimensional
610 acoustic visualization of zooplankton patchiness. *Deep Sea Research Part II: Topical Studies in Oceanography*, 45
611 (7):1201–1217, 1998.
- 612 Charles F Greenlaw. Acoustical estimation of zooplankton populations 1. *Limnology and Oceanography*, 24(2):
613 226–242, 1979.
- 614 Davide Guerra, Katrin Schroeder, Mireno Borghini, Elisa Camatti, Marco Pansera, Anna Schroeder, Stefania
615 Sparnocchia, and Jacopo Chiggiato. Zooplankton diel vertical migration in the corsica channel (north-western
616 mediterranean sea) detected by a moored acoustic doppler current profiler. *Ocean Science*, 15(3):631–649, 2019.
- 617 James M Hamilton, Kate Collins, and Simon J Prinsenberg. Links between ocean properties, ice cover, and plankton
618 dynamics on interannual time scales in the canadian arctic archipelago. *Journal of Geophysical Research: Oceans*,
619 118(10):5625–5639, 2013.
- 620 Graeme C Hays. A review of the adaptive significance and ecosystem consequences of zooplankton diel vertical
621 migrations. In *Migrations and Dispersal of Marine Organisms: Proceedings of the 37 th European Marine Biology*
622 *Symposium held in Reykjavík, Iceland, 5–9 August 2002*, pages 163–170. Springer, 2003.
- 623 PJ Herring, MJR Fasham, AR Weeks, JCP Hemmings, HSJ Roe, PR Pugh, S Holley, NA Crisp, and MV Angel.
624 Across-slope relations between the biological populations, the euphotic zone and the oxygen minimum layer off
625 the coast of oman during the southwest monsoon (august, 1994). *Progress in Oceanography*, 41(1):69–109, 1998.
- 626 Karen J Heywood, S Scrope-Howe, and ED Barton. Estimation of zooplankton abundance from shipborne adcp
627 backscatter. *Deep Sea Research Part A. Oceanographic Research Papers*, 38(6):677–691, 1991.
- 628 Laura Hobbs, Neil S Banas, Jonathan H Cohen, Finlo R Cottier, Jørgen Berge, and Øystein Varpe. A marine
629 zooplankton community vertically structured by light across diel to interannual timescales. *Biology Letters*, 17(2):
630 20200810, 2021.
- 631 Raleigh R Hood, Lynnath E Beckley, and Jerry D Wiggert. Biogeochemical and ecological impacts of boundary
632 currents in the indian ocean. *Progress in Oceanography*, 156:290–325, 2017.
- 633 Raleigh R Hood, Victoria J Coles, Jenny A Huggett, Michael R Landry, Marina Levy, James W Moffett, and Timothy
634 Rixen. Nutrient, phytoplankton, and zooplankton variability in the indian ocean. In *The Indian Ocean and its*
635 *role in the global climate system*, pages 293–327. Elsevier, 2024.

- 636 Ryuichiro Inoue, Minoru Kitamura, and Tetsuichi Fujiki. Diel vertical migration of zooplankton at the s 1 biogeo-
637 chemical mooring revealed from acoustic backscattering strength. *Journal of Geophysical Research: Oceans*, 121
638 (2):1031–1050, 2016.
- 639 D. A. Jayakumar, Christopher A. Francis, S.W.A. Naqvi, and Bess B. Ward. Diversity of nitrite reductase genes
640 (nirs) in the denitrifying water column of the coastal arabian sea. *Aquatic Microbial Ecology*, 2004. doi: 10.3354/
641 ame034069.
- 642 Songnian Jiang, Tommy D Dickey, Deborah K Steinberg, and Laurence P Madin. Temporal variability of zooplankton
643 biomass from adcp backscatter time series data at the bermuda testbed mooring site. *Deep Sea Research Part I:*
644 *Oceanographic Research Papers*, 54(4):608–636, 2007.
- 645 R Jyothibabu, NV Madhu, H Habeebrehman, KV Jayalakshmy, KKC Nair, and CT Achuthankutty. Re-evaluation
646 of ‘paradox of mesozooplankton’ in the eastern arabian sea based on ship and satellite observations. *Journal of*
647 *Marine Systems*, 81(3):235–251, 2010.
- 648 Myounghee Kang, Sunyoung Oh, Wooseok Oh, Dong-Jin Kang, SungHyun Nam, and Kyoungsoon Lee. Acoustic
649 characterization of fish and macroplankton communities in the seychelles-chagos thermocline ridge of the southwest
650 indian ocean. *Deep Sea Research Part II: Topical Studies in Oceanography*, 213:105356, 2024.
- 651 Madhavan Girijakumari Keerthi, Matthieu Lengaigne, Marina Levy, Jerome Vialard, Vallivattathillam Parvathi,
652 Clément de Boyer Montégut, Christian Ethé, Olivier Aumont, Iyyappan Suresh, Valiya Parambil Akhil, et al.
653 Physical control of interannual variations of the winter chlorophyll bloom in the northern arabian sea. *Biogeosciences*, 14(15):3615–3632, 2017.
- 655 Punam A Khandagale, Vaibhav D Mhatre, and Sujitha Thomas. Seasonal and spatial variability of zooplankton
656 diversity in north eastern arabian sea along the maharashtra coast. *Journal of the Marine Biological Association*
657 *of India*, 64(1):25–32, 2022.
- 658 S Kidwai and S Amjad. Zooplankton: pre-southwest and northeast monsoons of 1993 to 1994, from the north arabian
659 sea. *Mar. Biol.*, 136(3):561–571, apr 2000.
- 660 S. Prasanna Kumar, M. Madhupratap, M. Dileep Kumar, Mangesh Gauns, P.M. Muraleedharan, V. V. S. S. Sarma,
661 and Sílvia Naves de Souza. Physical control of primary productivity on a seasonal scale in central and eastern
662 arabian sea. *Journal of Earth System Science*, 2000. doi: 10.1007/bf02708331.
- 663 Michael R Landry. Grazing processes and secondary production in the arabian sea: A simple food web synthesis
664 with measurement constraints. In *Indian Ocean Biogeochemical Processes and Ecological Variability*, Geophysical
665 monograph, pages 133–146. American Geophysical Union, Washington, D. C., 2009.
- 666 Corinne Le Qu, Robbie M Andrew, Josep G Canadell, Stephen Sitch, Jan Ivar Korsbakken, Glen P Peters, Andrew C
667 Manning, Thomas A Boden, Pieter P Tans, Richard A Houghton, et al. Global carbon budget 2016. *Earth System*
668 *Science Data*, 8(2):605–649, 2016.

- 669 Marina Lévy, D Shankar, J-M André, SSC Shenoi, Fabien Durand, and Clément de Boyer Montégut. Basin-wide
670 seasonal evolution of the indian ocean's phytoplankton blooms. *Journal of Geophysical Research: Oceans*, 112
671 (C12), 2007.
- 672 M Li, A Gargett, and K Denman. What determines seasonal and interannual variability of phytoplankton and
673 zooplankton in strongly estuarine systems? *Estuarine, Coastal and Shelf Science*, 50(4):467–488, 2000.
- 674 Yanliang Liu, Jingsong Guo, Yuhuan Xue, Chalermrat Sangmanee, Huiwu Wang, Chang Zhao, Somkiat Khokiat-
675 tiwong, and Weidong Yu. Seasonal variation in diel vertical migration of zooplankton and micronekton in the
676 andaman sea observed by a moored adcp. *Deep Sea Research Part I: Oceanographic Research Papers*, 179:103663,
677 2022.
- 678 Alan R Longhurst and Warren S Wooster. Abundance of oil sardine (*sardinella longiceps*) and upwelling on the
679 southwest coast of india. *Can. J. Fish. Aquat. Sci.*, 47(12):2407–2419, dec 1990.
- 680 M Madhupratap, P Haridas, Neelam Ramaiah, and CT Achuthankutty. Zooplankton of the southwest coast of india:
681 abundance, composition, temporal and spatial variability in 1987. 1992.
- 682 M Madhupratap, TC Gopalakrishnan, P Haridas, KKC Nair, PN Aravindakshan, G Padmavati, and Shiney Paul.
683 Lack of seasonal and geographic variation in mesozooplankton biomass in the arabian sea and its structure in the
684 mixed layer. *Current science. Bangalore*, 71(11):863–868, 1996a.
- 685 M Madhupratap, S Prasanna Kumar, PMA Bhattathiri, M Dileep Kumar, S Raghukumar, KKC Nair, and N Rama-
686 iah. Mechanism of the biological response to winter cooling in the northeastern arabian sea. *Nature*, 384(6609):
687 549–552, 1996b.
- 688 M Madhupratap, TC Gopalakrishnan, P Haridas, and KKC Nair. Mesozooplankton biomass, composition and
689 distribution in the arabian sea during the fall intermonsoon: implications of oxygen gradients. *Deep Sea Research
690 Part II: Topical Studies in Oceanography*, 48(6-7):1345–1368, 2001.
- 691 PA Maheswaran, G Rajesh, C Revichandran, and KKC Nair. Upwelling and associated hydrography along the west
692 coast of india during southwest monsoon, 1999. 2000.
- 693 John Marra and Richard T. Barber. Primary productivity in the arabian sea: A synthesis of jgofs data. *Progress
694 in Oceanography*, 65(2):159–175, 2005. ISSN 0079-6611. doi: <https://doi.org/10.1016/j.pocean.2005.03.004>. URL
695 <https://www.sciencedirect.com/science/article/pii/S007966110500042X>. The Arabian Sea of the 1990s: New
696 Biogeochemical Understanding.
- 697 JP McCreary, Raghu Murtugudde, Jerome Vialard, PN Vinayachandran, Jerry D Wiggert, Raleigh R Hood,
698 D Shankar, and S Shetye. Biophysical processes in the indian ocean. *Indian Ocean biogeochemical processes
699 and ecological variability*, 185:9–32, 2009.
- 700 Julian P McCreary Jr, Pijush K Kundu, and Robert L Molinari. A numerical investigation of dynamics, thermody-
701 namics and mixed-layer processes in the indian ocean. *Progress in Oceanography*, 31(3):181–244, 1993.

- 702 Donald C McNaught. Acoustical determination of zooplankton distribution. In *Proc. 11th Conf. Great lakes Res.*,
703 pages 76–84, 1968.
- 704 John M Morrison, LA Codispoti, S Gaurin, Burton Jones, V Manghnani, and Z Zheng. Seasonal variation of
705 hydrographic and nutrient fields during the us jgofs arabian sea process study. *Deep Sea Research Part II: Topical*
706 *Studies in Oceanography*, 45(10-11):2053–2101, 1998.
- 707 A Mukherjee, D Shankar, V Fernando, P Amol, SG Aparna, R Fernandes, GS Michael, ST Khalap, NP Satelkar,
708 Y Agarvadekar, et al. Observed seasonal and intraseasonal variability of the east india coastal current on the
709 continental slope. *Journal of Earth System Science*, 123(6):1197–1232, 2014.
- 710 S Mukhopadhyay, D Shankar, SG Aparna, A Mukherjee, V Fernando, A Kankonkar, S Khalap, NP Satelkar,
711 MG Gaonkar, AP Tari, et al. Observed variability of the east india coastal current on the continental slope
712 during 2009–2018. *Journal of Earth System Science*, 129:1–22, 2020.
- 713 Jerry Mullison. Backscatter estimation using broadband acoustic doppler current profilers-updated. In *Proceedings*
714 *of the ASCE Hydraulic Measurements & Experimental Methods Conference, Durham, NH, USA*, pages 9–12,
715 2017.
- 716 KKC Nair, M Madhupratap, TC Gopalakrishnan, P Haridas, and Mangesh Gauns. The arabian sea: physical
717 environment, zooplankton and myctophid abundance. 1999.
- 718 PV Nair. Primary productivity in the indian seas. *CMFRIBulletin*, 22:1–63, 1970.
- 719 D Nethery and D Shankar. Vertical propagation of baroclinic kelvin waves along the west coast of india. *J. Earth*
720 *Syst. Sci.*, 116(4):331–339, aug 2007.
- 721 Lingyun Nie, Jianchao Li, Hao Wu, Wenchao Zhang, Yongjun Tian, Yang Liu, Peng Sun, Zhenjiang Ye, Shuyang
722 Ma, and Qinfeng Gao. The influence of ocean processes on fine-scale changes in the yellow sea cold water mass
723 boundary area structure based on acoustic observations. *Remote Sensing*, 15(17):4272, 2023.
- 724 MD Ohman and H-J Hirche. Density-dependent mortality in an oceanic copepod population. *Nature*, 412(6847):
725 638–641, 2001.
- 726 G Padmavati, P Haridas, KKC Nair, TC Gopalakrishnan, P Shiney, and M Madhupratap. Vertical distribution of
727 mesozooplankton in the central and eastern arabian sea during the winter monsoon. *Journal of Plankton Research*,
728 20(2):343–354, 1998.
- 729 MR Patil, CP Ramamirtham, P Udaya Varma, and CP Nair. Hydrography of the west coast of india during the
730 pre-monsoon period of the year 1962. *Journal of marine biological association of India*, 6(1):151–164, 1964.
- 731 Richard Edward Pieper. *A study of the relationship between zooplankton and high-frequency scattering of underwater*
732 *sound*. PhD thesis, University of British Columbia, 1971.

- 733 SA Piontkovski, R Williams, and TA Melnik. Spatial heterogeneity, biomass and size structure of plankton of the
734 indian ocean: some general trends. *Marine ecology progress series*, pages 219–227, 1995.
- 735 Emmanuel Potiris, Constantin Frangoulis, Alkiviadis Kalampokis, Manolis Ntoumas, Manos Pettas, George Peti-
736 hakis, and Vassilis Zervakis. Acoustic doppler current profiler observations of migration patterns of zooplankton
737 in the cretan sea. *Ocean Science*, 14(4):783–800, 2018.
- 738 SZ Qasim. Biological productivity of the indian ocean. 1977.
- 739 CP Ramamirtham and AVS Murty. Hydrography of the west coast of india during the pre-monsoon period of the
740 year 1962—part 2: in and offshore waters of the konkan and malabar coasts. *Journal of the Marine Biological
741 Association of India*, 7(1):150–168, 1965.
- 742 S Ramamurthy. Studies on the plankton of the north kanara coast in relation to the pelagic fishery. *Journal of
743 Marine Biological Association of India*, 7(1):127–149, 1965.
- 744 M Reckermann and M J W Veldhuis. Trophic interactions between picophytoplankton and micro- and nanozoo-
745 plankton in the western arabian sea during the NE monsoon 1993. *Aquat. Microb. Ecol.*, 12:263–273, 1997.
- 746 Mehbuba Rehim and Mudassar Imran. Dynamical analysis of a delay model of phytoplankton–zooplankton interac-
747 tion. *Applied Mathematical Modelling*, 36(2):638–647, 2012.
- 748 T. P. Rippeth and J. H. Simpson. Diurnal signals in vertical motions on the hebridean shelf. *Limnology and
749 Oceanography*, 43:1690–1696, 1998. doi: 10.4319/lo.1998.43.7.1690.
- 750 William J Ripple, James A Estes, Oswald J Schmitz, Vanessa Constant, Matthew J Kaylor, Adam Lenz, Jennifer L
751 Motley, Katharine E Self, David S Taylor, and Christopher Wolf. What is a trophic cascade? *Trends Ecol. Evol.*,
752 31(11):842–849, November 2016.
- 753 John H Ryther, John R Hall, Allan K Pease, Andrew Bakun, and Mark M Jones. Primary organic production in
754 relation to the chemistry and hydrography of the western indian ocean 1. *Limnology and Oceanography*, 11(3):
755 371–380, 1966.
- 756 D Sameoto and S Paulowich. The use of 120 khz sonar in zooplankton studies. In *OCEANS'77 Conference Record*,
757 pages 523–528. IEEE, 1977.
- 758 VVSS Sarma, TVS Udaya Bhaskar, J Pavan Kumar, and Kunal Chakraborty. Potential mechanisms responsible for
759 occurrence of core oxygen minimum zone in the north-eastern arabian sea. *Deep Sea Research Part I: Oceano-
760 graphic Research Papers*, 165:103393, 2020.
- 761 Friedrich A. Schott and Julian P. McCreary. The monsoon circulation of the indian ocean. *Progress in Oceanography*,
762 51(1):1–123, 2001. ISSN 0079-6611. doi: [https://doi.org/10.1016/S0079-6611\(01\)00083-0](https://doi.org/10.1016/S0079-6611(01)00083-0). URL <https://www.sciencedirect.com/science/article/pii/S0079661101000830>.

- 764 D Shankar and SR Shetye. On the dynamics of the lakshadweep high and low in the southeastern arabian sea.
765 *Journal of Geophysical Research: Oceans*, 102(C6):12551–12562, 1997.
- 766 D Shankar, R Remya, PN Vinayachandran, Abhisek Chatterjee, and Ambica Behera. Inhibition of mixed-layer
767 deepening during winter in the northeastern arabian sea by the west india coastal current. *Climate Dynamics*,
768 47:1049–1072, 2016.
- 769 D Shankar, R Remya, AC Anil, and V Vijith. Role of physical processes in determining the nature of fisheries in the
770 eastern arabian sea. *Progress in Oceanography*, 172:124–158, 2019.
- 771 SR Shetye and AD Gouveia. Coastal circulation in the north indian ocean: Coastal segment (14, sw). John Wiley
772 and Sons, New York, USA, 1998.
- 773 SR Shetye, AD Gouveia, SSC Shenoi, D Sundar, GS Michael, AM Almeida, and K Santanam. Hydrography and
774 circulation off the west coast of india during the southwest monsoon 1987. 1990.
- 775 SR Shetye, AD Gouveia, SSC Shenoi, GS Michael, D Sundar, AM Almeida, and K Santanam. The coastal current
776 off western india during the northeast monsoon. *Deep Sea Research Part A. Oceanographic Research Papers*, 38
777 (12):1517–1529, 1991.
- 778 SR Shetye, AD Gouveia, and SSC Shenoi. Does winter cooling lead to the subsurface salinity minimum off saurashtra,
779 india? *Oceanography of the Indian Ocean*, pages 617–625, 1992.
- 780 Wei Shi and Menghua Wang. Phytoplankton biomass dynamics in the arabian sea from viirs observations. *Journal
781 of Marine Systems*, 227:103670, 2022.
- 782 Wei Shi, John M Morrison, Emanuele Böhm, and Vijayakumar Manghnani. Remotely sensed features in the us jgofs
783 arabian sea process study. *Deep Sea Research Part II: Topical Studies in Oceanography*, 46(8-9):1551–1575, 1999.
- 784 Houssem Smeti, Marc Pagano, Christophe Menkes, Anne Lebourges-Dhaussy, Brian PV Hunt, Valerie Allain, Martine
785 Rodier, Florian De Boissieu, Elodie Kestenare, and Cherif Sammari. Spatial and temporal variability of zooplankton
786 off n ew c aledonia (s outhwestern p acific) from acoustics and net measurements. *Journal of Geophysical
787 Research: Oceans*, 120(4):2676–2700, 2015.
- 788 Sharon Smith, Michael Roman, Irina Prusova, Karen Wishner, Marcia Gowing, LA Codispoti, Richard Barber, John
789 Marra, and Charles Flagg. Seasonal response of zooplankton to monsoonal reversals in the arabian sea. *Deep Sea
790 Research Part II: Topical Studies in Oceanography*, 45(10-11):2369–2403, 1998.
- 791 SL Smith and M Madhupratap. Mesozooplankton of the arabian sea: patterns influenced by seasons, upwelling, and
792 oxygen concentrations. *Progress in Oceanography*, 65(2-4):214–239, 2005.
- 793 Patnaik Sreenivas, KVKRK Patnaik, and KVSR Prasad. Monthly variability of mixed layer over arabian sea using
794 argo data. *Marine Geodesy*, 31(1):17–38, 2008.

- 795 R Subrahmanyam. Studies on the phytoplankton of the west coast of india: Part ii. physical and chemical factors
796 influencing the production of phytoplankton, with remarks on the cycle of nutrients and on the relationship of
797 the phosphate-content to fish landings. In *Proceedings/Indian Academy of Sciences*, volume 50, pages 189–252.
798 Springer, 1959.
- 799 R Subrahmanyam and AH Sarma. Studies on the phytoplankton of the west coast of india. part iii. seasonal variation
800 of the phytoplankters and environmental factors. *Indian Journal of Fisheries*, 7(2):307–336, 1960.
- 801 V. Sudheesh, G.V.M. Gupta, Yudhishtir Reddy, Kausar F. Bepari, N.V.H.K. Chari, C.K. Sherin, S.S. Shaju, Ch.V.
802 Ramu, and Anil Kumar Vijayan. Oxygen minimum zone along the eastern arabian sea: Intra-annual varia-
803 tion and dynamics based on ship-borne studies. *Progress in Oceanography*, 201:102742, 2022. ISSN 0079-6611.
804 doi: <https://doi.org/10.1016/j.pocean.2022.102742>. URL <https://www.sciencedirect.com/science/article/pii/S0079661122000040>.
- 805 Laura Ursella, Vanessa Cardin, Mirna Batistić, Rade Garić, and Miroslav Gačić. Evidence of zooplankton vertical
806 migration from continuous southern adriatic buoy current-meter records. *Progress in oceanography*, 167:78–96,
807 2018.
- 808 Laura Ursella, Sara Pensieri, Enric Pallàs-Sanz, Sharon Z Herzka, Roberto Bozzano, Miguel Tenreiro, Vanessa Cardin,
809 Julio Candela, and Julio Sheinbaum. Diel, lunar and seasonal vertical migration in the deep western gulf of mexico
810 evidenced from a long-term data series of acoustic backscatter. *Progress in Oceanography*, 195:102562, 2021.
- 811 V Vijith, PN Vinayachandran, V Thushara, P Amol, D Shankar, and AC Anil. Consequences of inhibition of mixed-
812 layer deepening by the west india coastal current for winter phytoplankton bloom in the northeastern arabian sea.
813 *Journal of Geophysical Research: Oceans*, 121(9):6583–6603, 2016.
- 814 Peter H Wiebe, Charles H Greene, Timothy K Stanton, and Janusz Burczynski. Sound scattering by live zooplankton
815 and micronekton: empirical studies with a dual-beam acoustical system. *The Journal of the Acoustical Society of
816 America*, 88(5):2346–2360, 1990.
- 817 Monika Winder and Daniel E Schindler. Climatic effects on the phenology of lake processes. *Global change biology*,
818 10(11):1844–1856, 2004.
- 819 Karen F Wishner, Marcia M Gowing, and Celia Gelfman. Mesozooplankton biomass in the upper 1000 m in the
820 arabian sea: overall seasonal and geographic patterns, and relationship to oxygen gradients. *Deep Sea Research
821 Part II: Topical Studies in Oceanography*, 45(10-11):2405–2432, 1998.

Table 1: ADCP deployment details at the locations. The temporal resolution is 1 hour, bin size(vertical resolution) 4 m. All ADCPs are operated at 153.3 kHz. The moorings are at a water column depth of 950 – 1200 m on the continental slope and are serviced on yearly basis according to ship availability. The 6th column consists of Reference echo intensity (Er) for each beam, while the 7th column contains the corresponding RSSI conversion factor [Deines, 1999].

Station (Position; $^{\circ}$ E, $^{\circ}$ N)	Date		Depth			
	Deployment	Recovery	Ocean	ADCP	Er	Kc
Okha (67.47, 22.26)	01/10/2018	01/12/2019	996	118	37 , 37 , 37 , 36	0.42 , 0.44 , 0.42 , 0.43
	01/12/2019	04/12/2020	1166	312	39 , 36 , 38 , 36	0.42 , 0.44 , 0.42 , 0.43
	04/12/2020	08/03/2022	1021	144	41 , 37 , 38 , 37	0.42 , 0.44 , 0.42 , 0.43
	08/03/2022	01/01/2023	1019	142	37 , 38 , 39 , 36	0.42 , 0.44 , 0.42 , 0.43
Mumbai (69.24, 20.01)	09/11/2017	29/09/2018	1025	150	36 , 34 , 39 , 42	0.40 , 0.40 , 0.40 , 0.40
	29/09/2018	29/11/2019	1122	125	35 , 36 , 39 , 42	0.40 , 0.40 , 0.40 , 0.40
	29/11/2019	02/12/2020	1143	164	37 , 34 , 39 , 43	0.40 , 0.40 , 0.40 , 0.40
	02/12/2020	06/03/2022	1125	142	36 , 34 , 39 , 42	0.40 , 0.40 , 0.40 , 0.40
	07/03/2022	02/01/2023	1103	158	37 , 34 , 40 , 43	0.40 , 0.40 , 0.40 , 0.40
Jaigarh (71.12, 17.53)	27/10/2017	27/09/2018	1039	198	32 , 35 , 33 , 32	0.45 , 0.45 , 0.45 , 0.45
	27/09/2018	30/10/2019	1032	164	32 , 35 , 33 , 31	0.45 , 0.45 , 0.45 , 0.45
	03/11/2019	30/11/2020	1142	264	32 , 36 , 33 , 32	0.45 , 0.45 , 0.45 , 0.45
	30/11/2020	05/03/2022	1099	119	33 , 36 , 34 , 32	0.45 , 0.45 , 0.45 , 0.45
Goa (72.74, 15.17)	03/10/2017	25/09/2018	1000	174	35 , 37 , 34 , 35	0.44 , 0.44 , 0.40 , 0.41
	25/09/2018	16/10/2019	969	145	38 , 36 , 36 , 34	0.44 , 0.44 , 0.40 , 0.41
	16/10/2019	29/11/2020	966	143	44 , 38 , 36 , 43	0.44 , 0.44 , 0.40 , 0.41
	29/11/2020	03/03/2022	985	157	35 , 40 , 35 , 38	0.44 , 0.44 , 0.40 , 0.41
	03/03/2022	05/01/2023	984	159	35 , 38 , 35 , 34	0.44 , 0.44 , 0.40 , 0.41
Udupi (74.04, 12.5)	05/10/2017	06/10/2018	1028	176	44 , 46 , 29 , 35	0.45 , 0.45 , 0.45 , 0.45
	06/10/2018	18/10/2019	1027	179	32 , 38 , 30 , 36	0.45 , 0.45 , 0.45 , 0.45
	18/10/2019	11/12/2020	1018	168	33 , 37 , 31 , 38	0.45 , 0.45 , 0.45 , 0.45
	11/03/2022	06/01/2023	1036	155	31 , 32 , 32 , 33	0.45 , 0.45 , 0.45 , 0.45
Kollam (75.44, 9.05)	07/10/2017	08/10/2018	1174	200	43 , 55 , 45 , 43	0.49 , 0.50 , 0.49 , 0.50
	08/10/2018	20/10/2019	1160	123	49 , 62 , 46 , 46	0.49 , 0.50 , 0.49 , 0.50
	20/10/2019	13/12/2020	1209	176	52 , 61 , 54 , 55	0.49 , 0.50 , 0.49 , 0.50
	13/12/2020	13/03/2022	1129	91	49 , 51 , 46 , 47	0.49 , 0.50 , 0.49 , 0.50
	13/03/2022	08/01/2023	1149	164	41 , 48 , 43 , 41	0.49 , 0.50 , 0.49 , 0.50
Kanyakumari (77.39, 6.96)	16/11/2016	08/10/2017	1096	252	37 , 36 , 37 , 37	0.42 , 0.44 , 0.42 , 0.43
	08/10/2017	10/10/2018	1055	181	32 , 34 , 38 , 35	0.45 , 0.45 , 0.45 , 0.45
	10/10/2018	22/10/2019	1075	180	36 , 34 , 39 , 36	0.45 , 0.45 , 0.45 , 0.45
	22/10/2019	14/12/2020	1060	167	33 , 35 , 36 , 35	0.45 , 0.45 , 0.45 , 0.45
	14/12/2020	14/03/2022	1184	287	34 , 36 , 36 , 35	0.45 , 0.45 , 0.45 , 0.45

Table 2:

Volumetric samples of zooplankton of various stations. The sampling depth range is standardised for later years for bin range of 0–25m, 25–50m, 50–75m, 75–100m, 100–150m. The abbreviations are in the following manner: Okha (O), Mumbai (M), Jaigarh (J), Goa (G), Udupi (U), Kollam (K), Kanyakumari (KK); The number tags corresponds to particular cruise of a station.

Sample number	Tag	Lat($^{\circ}$ N)	Lon($^{\circ}$ E)	Date	Time (IST)	Sampling depth range (m)
1-3	G1	15.18	72.79	25 Sep 18	452	50–25, 100–50, 150–100
4-6	G2	15.16	72.71	25 Sep 18	2108	50–25, 100–50, 150–100
7-10	G2	15.16	72.71	25 Sep 18	2137	40–20, 60–40, 80–60, 100–80
11-14	J1			26 Sep 18	2000	40–20, 60–40, 80–60, 100–80
15-17	J2			27 Sep 18	2000	50–25, 100–50, 150–100
18-21	J2			27 Sep 18	2100	40–20, 60–40, 80–60, 100–80
22-25	M1	20	69.19	28 Sep 18	2135	40–20, 60–40, 80–60, 100–80
26-27	M1	20	69.19	28 Sep 18	2205	50–25, 100–50
28-29	M2	20.01	69.2	29 Sep 18	2035	50–25, 100–50
30-33	M2	20.01	69.2	29 Sep 18	2057	40–20, 60–40, 80–60, 100–80
34-37	U1			5 Oct 18	2000	40–20, 60–40, 80–60, 100–80
38-40	U1			5 Oct 18	2100	50–25, 100–50, 150–100
41-43	U2			6 Oct 18	2000	50–25, 100–50, 150–100
44-47	U2			6 Oct 18	2100	40–20, 60–40, 80–60, 100–80
48-51	K1	9.06	75.42	8 Oct 18	421	40–20, 60–40, 80–60, 100–80
52-54	K1	9.06	75.42	8 Oct 18	449	50–25, 100–50, 150–100
55-56	K2	9.04	75.4	8 Oct 18	2027	50–25, 100–50
57-60	K2	9.04	75.4	8 Oct 18	2045	40–20, 60–40, 80–60, 100–80
61-64	G2	15.16	72.74	16 Oct 19	829	50–25, 75–50, 100–75, 150–100
65-67	G3	15.16	72.74	16 Oct 19	1812	50–25, 75–50, 100–75
68-70	K2	9.02	75.42	20 Oct 19	840	50–25, 75–50, 100–75
71-74	K3	9.04	75.43	20 Oct 19	1934	50–25, 75–50, 100–75, 150–100
75-78	KK1			22 Oct 19	742	50–25, 75–50, 100–75, 150–100
79-82	KK2			22 Oct 19	1925	50–25, 75–50, 100–75, 150–100
83-86	J1			30 Oct 19	324	50–25, 75–50, 100–75, 150–100
87-89	J2			4 Nov 19	946	75–50, 100–75, 150–100
90-92	M2	19.98	69.22	29 Nov 19	1434	50–25, 75–50, 100–75
93-96	M3	20.01	69.23	30 Nov 19	958	50–25, 75–50, 100–75, 150–100
97-100	O1	22.24	67.49	1 Dec 19	937	50–25, 75–50, 100–75, 150–100
101	O2	22.25	67.46	1 Dec 19	1957	150–100
102-105	G3	15.68	73.22	28 Nov 20	930	50–25, 75–50, 100–75, 150–100
105-108	G4	15.32	73.22	29 Nov 20	1558	50–25, 75–50, 100–75, 150–100
108-110	J2	17.85	71.21	30 Nov 20	1458	75–50, 100–75, 150–100
111-114	J3	17.91	71.21	1 Dec 20	1052	50–25, 75–50, 100–75, 150–100
115-118	M4	20.03	69.38	2 Dec 20	2016	50–25, 75–50, 100–75, 150–100
119-00	O2	22.41	67.8	4 Dec 20	953	150–100
120-123	O3	22.41	67.79	4 Dec 20	2011	50–25, 75–50, 100–75, 150–100
124-127	K3	9.11	75.72	12 Dec 20	2335	50–25, 75–50, 100–75, 150–100
128-131	K4	9.06	75.74	13 Dec 20	1507	50–25, 75–50, 100–75, 150–100
132-134	KK1	7.62	77.63	14 Dec 20	1226	50–25, 75–50
135-138	KK2	7.62	77.63	14 Dec 20	2047	50–25, 75–50, 100–75, 150–100
139-142	G4	15.32	73.21	3 Mar 22	823	50–25, 75–50, 100–75, 150–100
143-146	G5	15.68	73.21	4 Mar 22	1030	50–25, 75–50, 100–75, 150–100
147-150	M5	19.99	69.23	7 Mar 22	957	50–25, 75–50, 100–75, 150–100
151-154	O3	22.24	67.5	8 Mar 22	806	50–25, 75–50, 100–75, 150–100
155-158	U3	12.5	74.04	12 Mar 22	1156	50–25, 75–50, 100–75, 150–100
159-160	K4	9.04	75.42	13 Mar 22	1027	50–25, 75–50, 100–75
161-164	KK3	6.97	77.4	15 Mar 22	1220	50–25, 75–50, 100–75, 150–100

Table 3:

The mean, standard deviation at 40 and 104 m of zooplankton biomass ($mg\ m^{-3}$), standard deviation of zooplankton standing stock ($mg\ m^{-2}$) and chlorophyll ($mg\ m^{-3}$) at 7 mooring sites are tabulated.

	40 m		104 m		decrease with depth (40 m - 104m)	standard deviation				
	Mean	Std	Mean	Std		Chl	ZSS	Intraseasonal	Intra-annual	Annual
Okha	230.42	22.84	151.68	25.58	78.74	0.25	1.93	64.26	63.78	22.38
Mumbai	272.86	34.95	182.24	30.34	90.62	0.13	2.9	70.74	83.52	41.58
Jaigarh	278.45	36.52	182.96	48.89	95.49	0.05	3.24	90.3	87.06	54.3
Goa	235.22	30.34	163.02	36.54	72.2	0.15	2.24	76.38	83.76	38.58
Udupi	247.81	34.37	169.37	38.8	78.43	0.55	2	77.22	100.86	41.64
Kollam	272.56	54.94	198.89	50.08	73.67	0.68	1.25	89.94	95.94	41.82
KanyaKumari	207.07	30.42	167.63	20.89	39.44	0.51	0.67	71.88	52.62	21.84

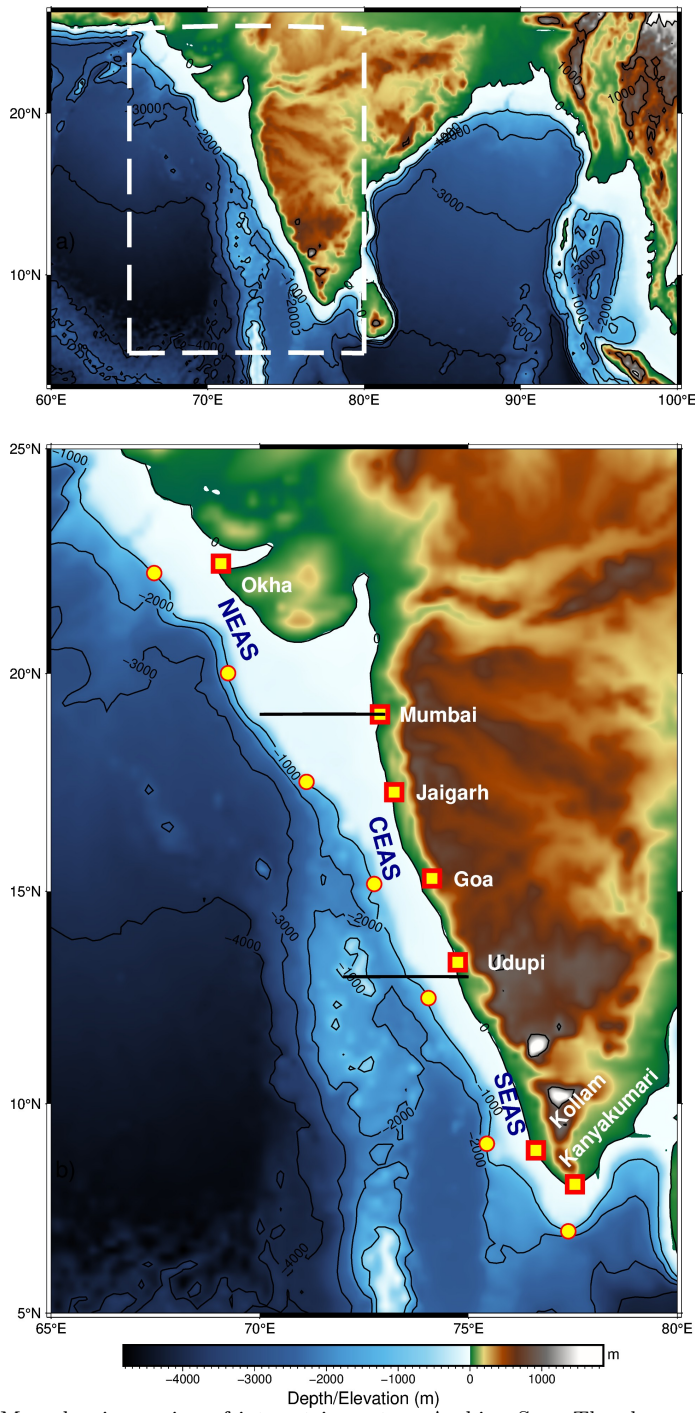


Figure 1: Map showing region of interest in eastern Arabian Sea. The slope moorings are deployed at ~ 1000 m depth as shown in the bathymetry contour. Note the increase in shelf width as we go poleward along the coast. The mooring sites off Okha and Mumbai are in Northern EAS; Jaigarh and Goa in Central EAS while Kollam and Kanyakumari are at Southern EAS. Udupi is situated at the transition zone of Central and Southern EAS.

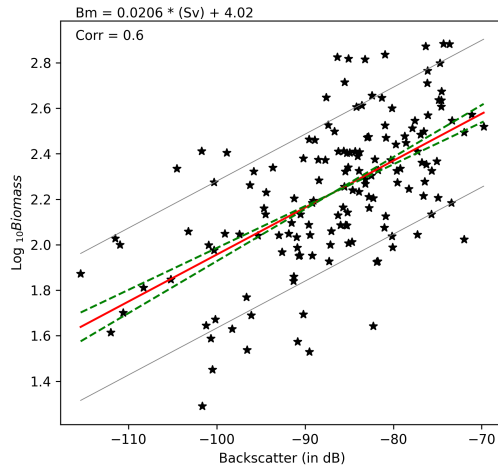


Figure 2: The linear fit line of Biomass (\log_{10} scale) and backscattering strength (in dB). The linear fit line is within the error range of previous result of [Aparna et al., 2022] (contained 67 data points) onto which latest zooplankton volumetric sample data (159 data points) is appended. The regression equation is $y = (0.02 \pm 0.0025)x + (4.0144 \pm 0.2198)$ and correlation value of 0.54. The dashed green lines denote error range of plausible slope and intercept. The first standard deviation of $\log_{10}(\text{Biomass})$ is ± 0.49 , which results in the backscatter range of 48.58 dB encompassing the entire backscatter range. It signifies the robustness of zooplankton biomass dependency on ADCP measured backscattering strength.

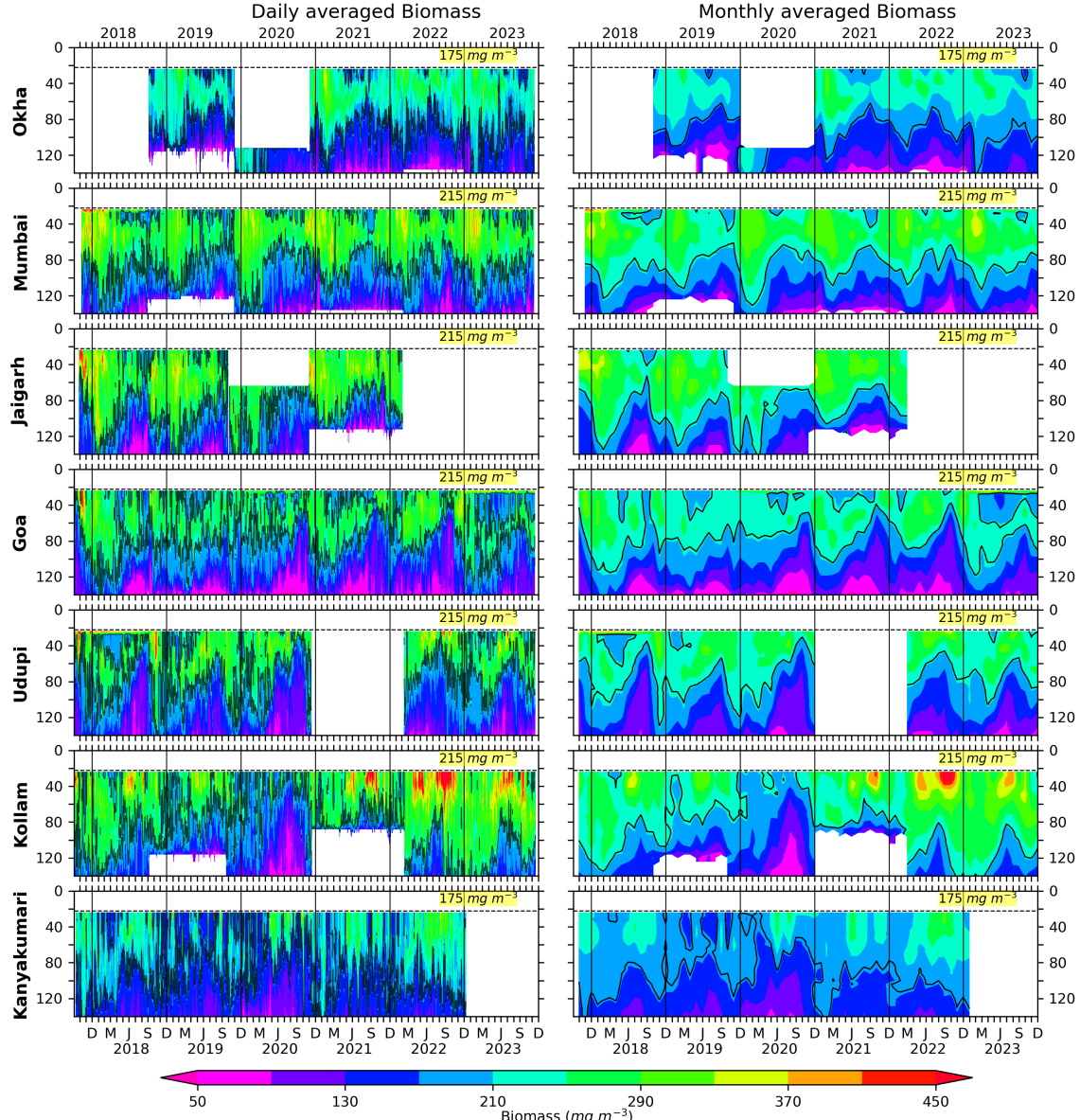


Figure 3: The Daily and monthly averaged biomass for EAS moorings, north (top) to south (bottom). The black contours are marking of 175 mg m^{-3} biomass for Okha and Kanyakumari; 215 mg m^{-3} for Mumbai, Goa and Kollam. The biomass contours are distinct and different based on the physico-chemical parameters and the one that best explains seasonality at respective location. The top 10 % of data is discarded due to echo noise. The dashed line at 22 m marks the top-depth of first bin i.e, 24 m.

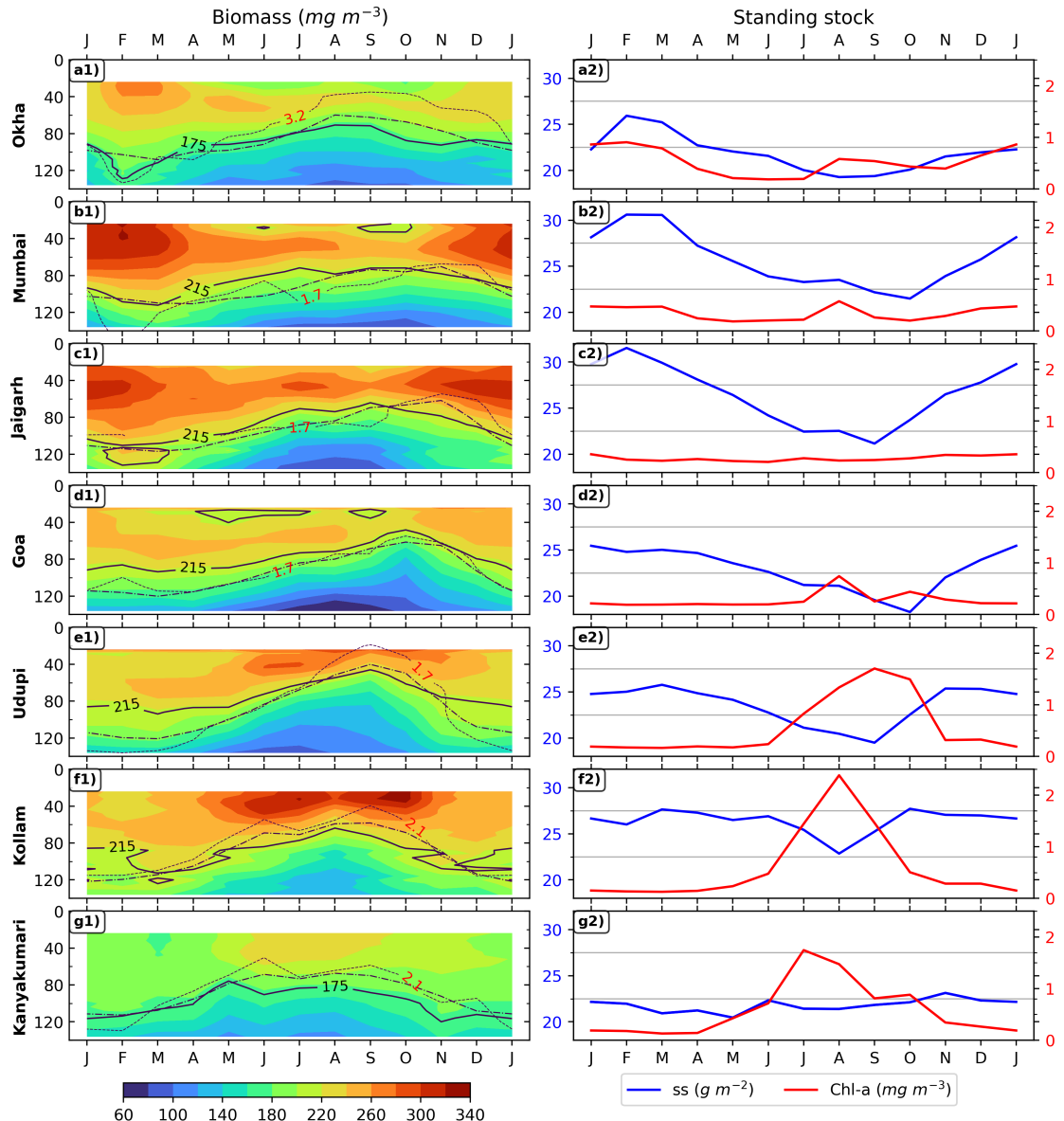


Figure 4: Monthly climatology of zooplankton biomass is shown in left panels for 7 locations, (top to bottom is southward). The D175 & D215 are shown in solid lines; dashed line represents the depth of 23 C isotherm; oxygen contours are shown in dotted lines and labeled for each mooring. The right set of panel plots is showing ZSS (24 – 140 biomass integral) and chlorophyll climatology for corresponding locations.

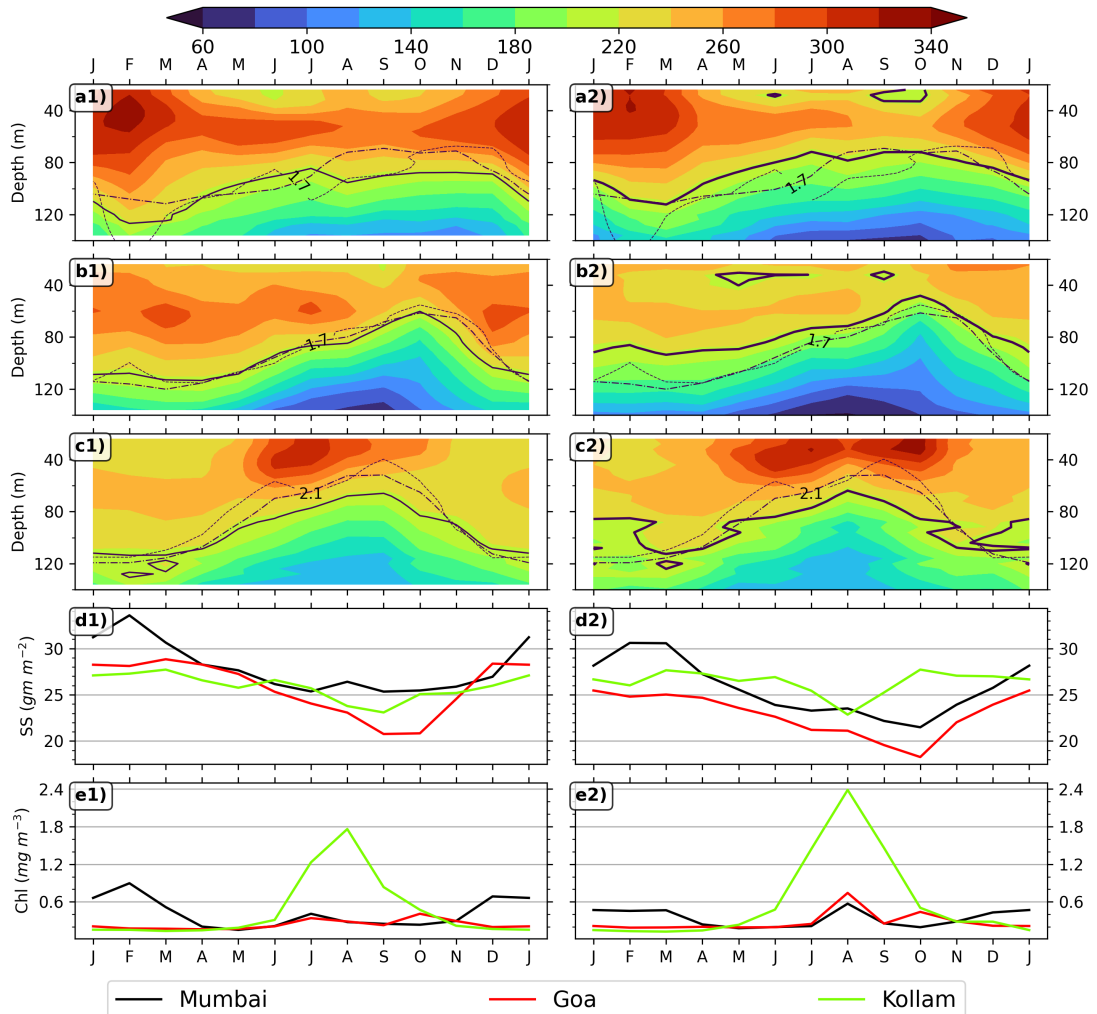


Figure 5: Monthly climatology of zooplankton biomass is shown in left panels for 3 locations which were earlier used in [Aparna et al., 2022]; a1, b1 & c1 is the biomass climatology for Mumbai, Goa and Kollam, d1 is for ZSS climatology (24 – 140 biomass integral), e1 is for chlorophyll biomass climatology; a2, b2, c2, d2 & e2 is same but based on data from 2017 to 2023. The D215 is shown in solid line. The dashed line represents the depth of 23 °C isotherm; oxygen contours are shown in dotted lines and labeled for each mooring.

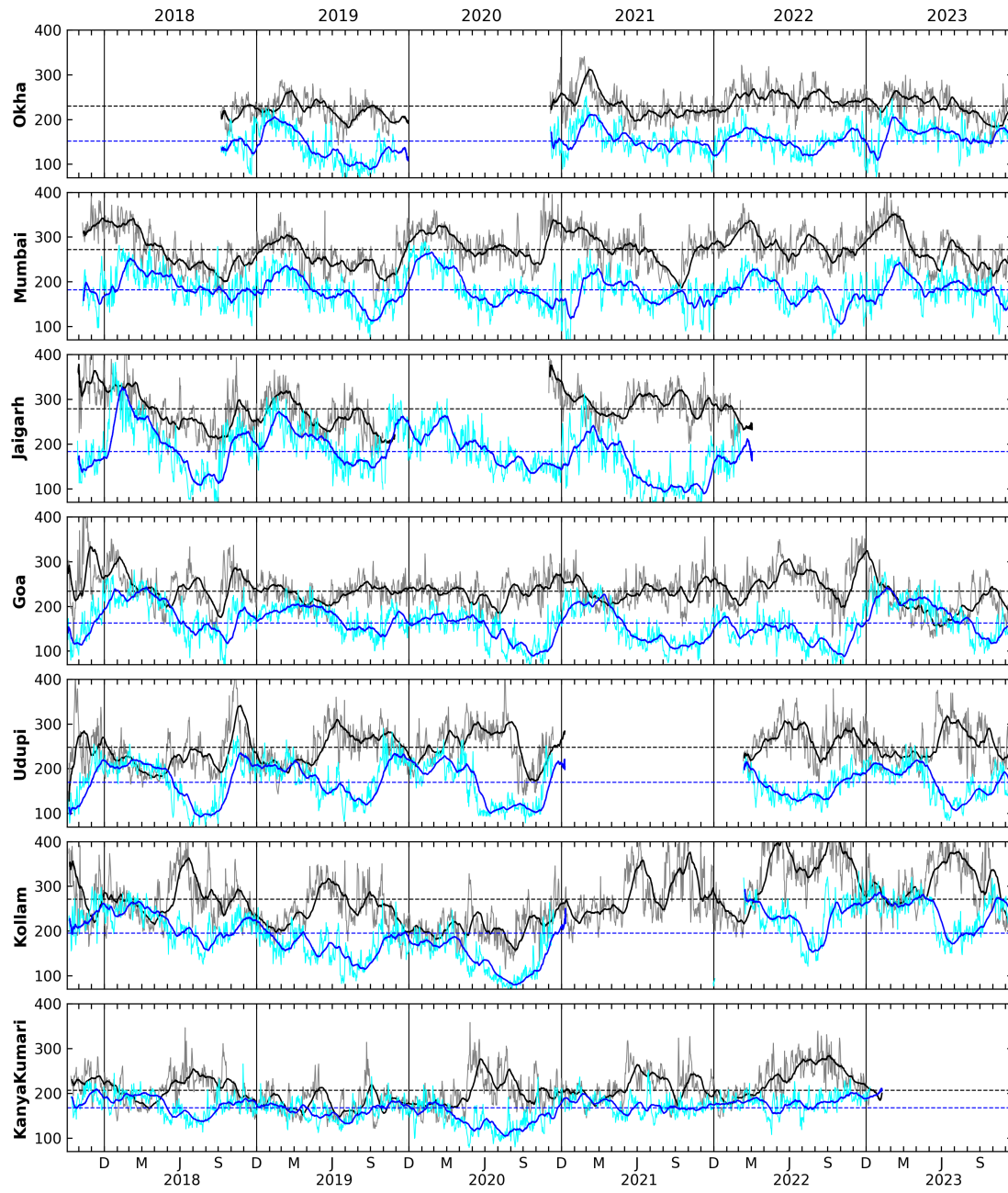


Figure 6: The daily biomass at depth of 40 m and 104 m for all locations shown by grey and cyan curves. The black and blue lines shows the 30 day rolling averaged biomass at 40 and 104 m, respectively. Notice the bursts seen in the daily data ranging from few days to weeks.

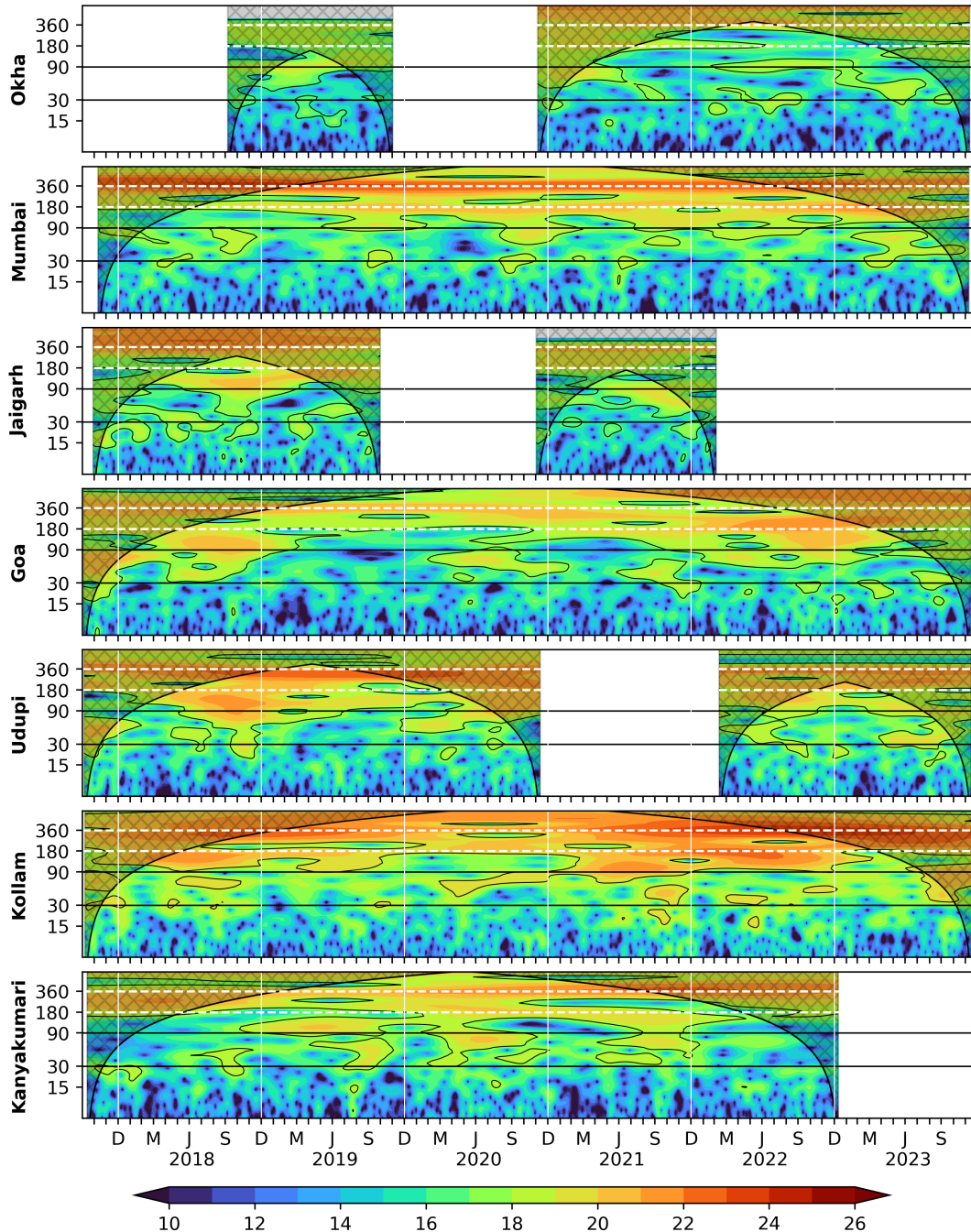


Figure 7: Wavelet power spectra (Morlet) of the 40 m zooplankton biomass plotted against time as abscissa and period in days as ordinate. The wavelet power is in \log_2 scale, the 95 % significance is marked in black contours; the cross-shaded region falls under cone of influence. Vertical white lines separates years.

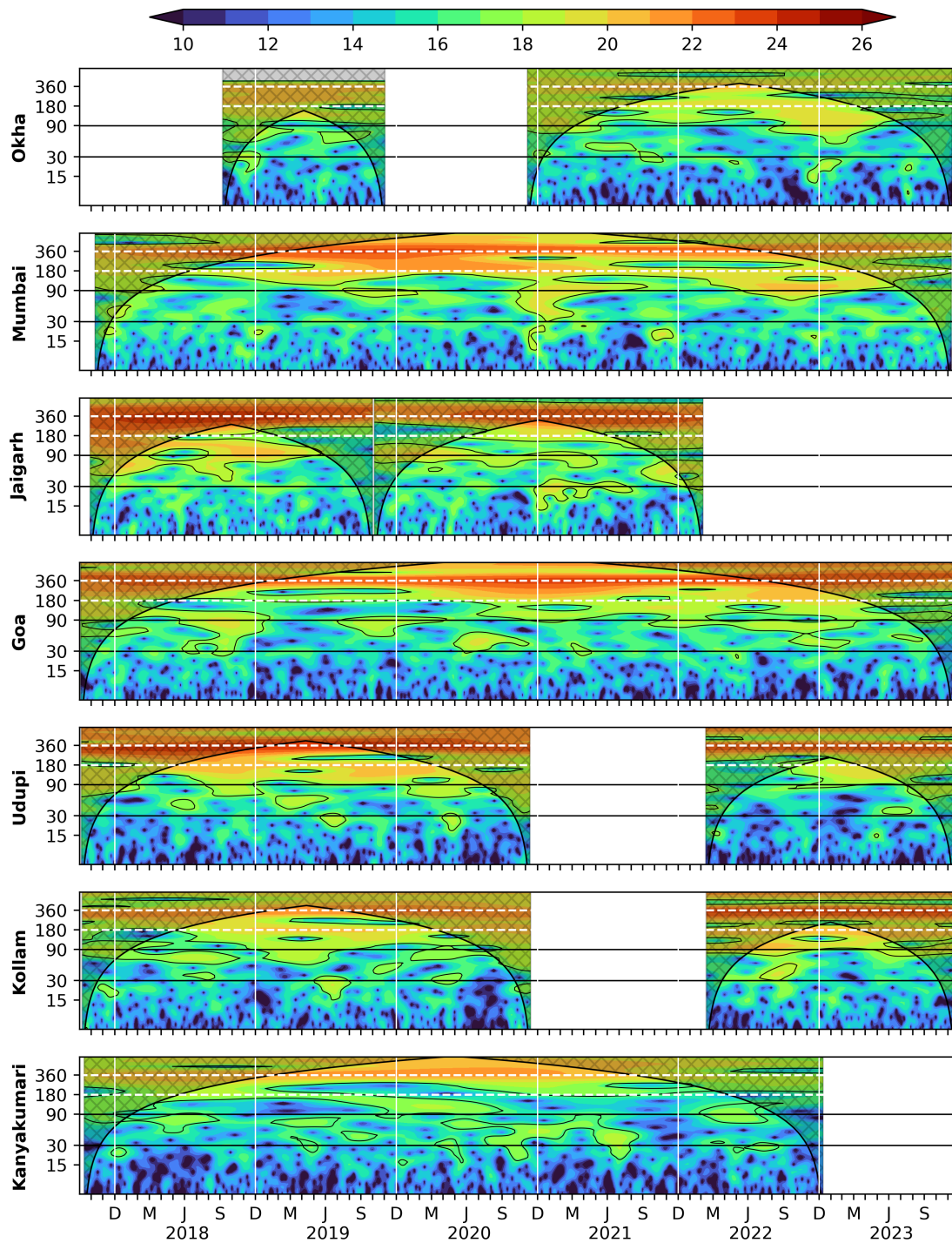


Figure 8: Wavelet power spectra (Morlet) of the 104 m zooplankton biomass plotted against time as abscissa and period in days as ordinate. The wavelet power is in \log_2 scale, the 95 % significance is marked in black contours; the cross-shaded region falls under cone of influence. The vertical white lines separates years.

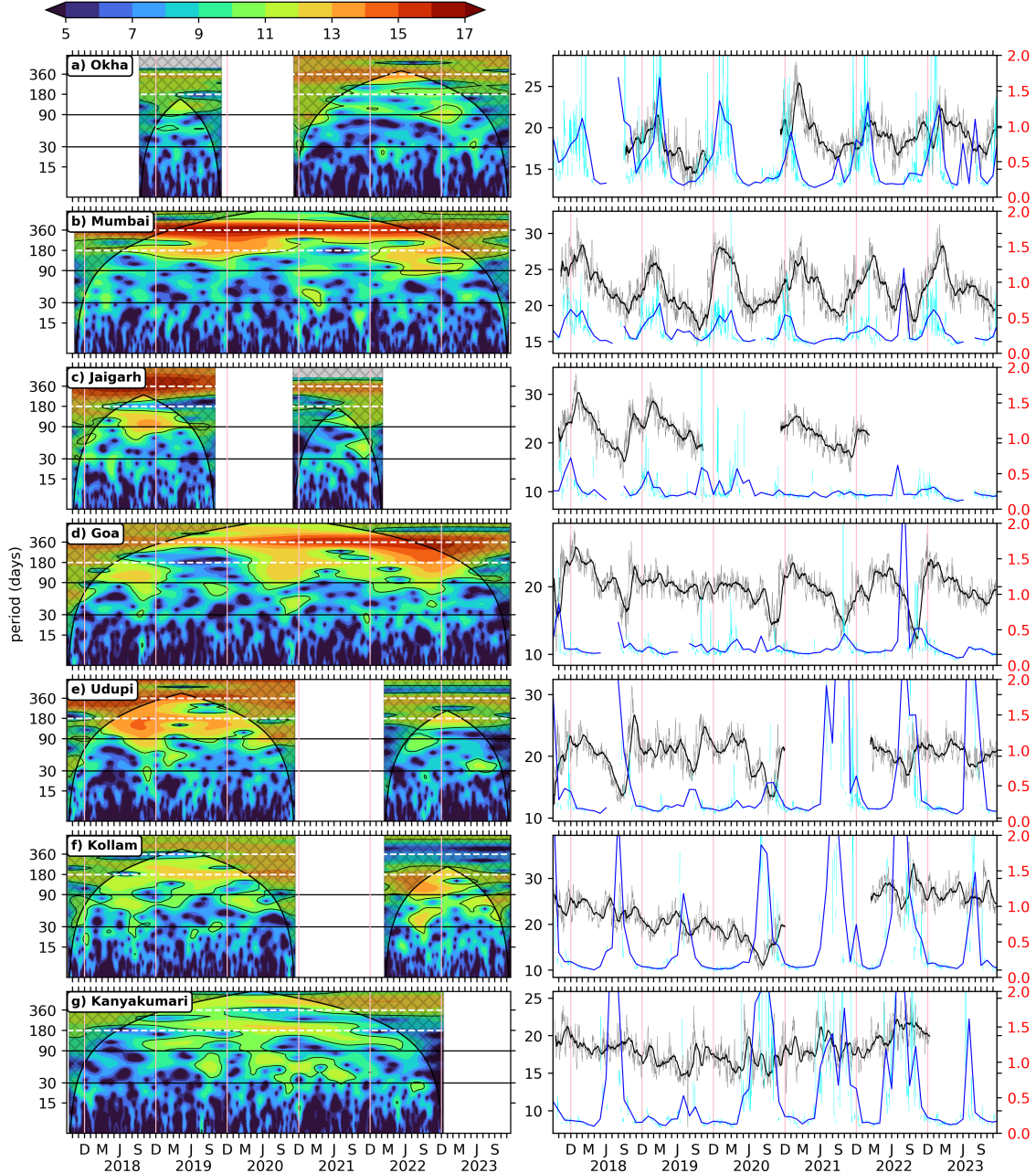


Figure 9: Wavelet power spectra (Morlet) of zooplankton standing stock plotted against time as abscissa and period in days as ordinate. The wavelet power is in log₂ scale, the 95 % significance is marked in black contours; The vertical white lines separates years. The right side panel shows the ZSS (24 – 120 m biomass integral) time series of 30 day rolling mean data (black) overlaid upon daily data (Grey). The 30 day rolling mean data of chlorophyll (solid blue) is plotted over its daily data (cyan).

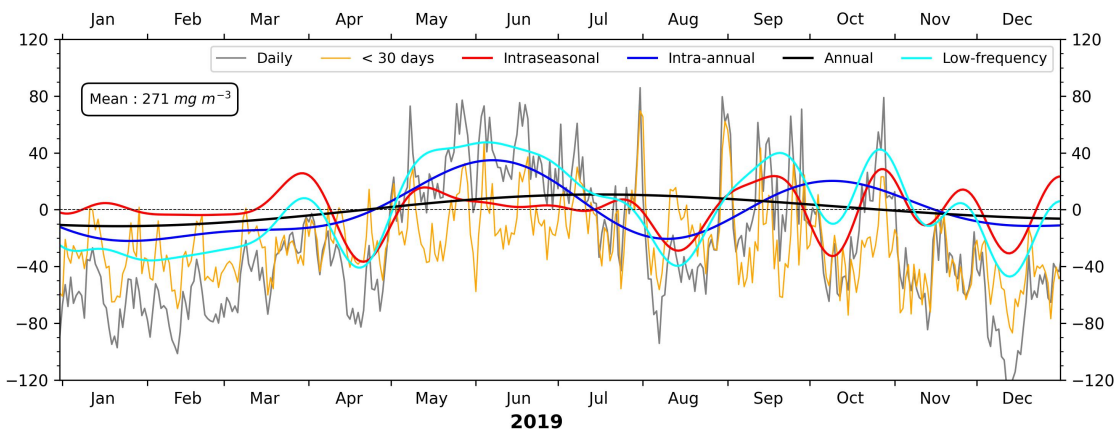


Figure 10: Comparison between mean-removed daily biomass time series at 40 m and the distinct components of variability off Kollam for 2019. The biomass units are $mg\ m^{-3}$. An increase in biomass is noticed from May onward and lasting till late monsoon with weeks of low biomass during August due to contribution from each component of variability. The cyan curve is sum of all low frequency components above 30 days, i.e, annual, intra-annual and 30 to 90 days intraseasonal variability.

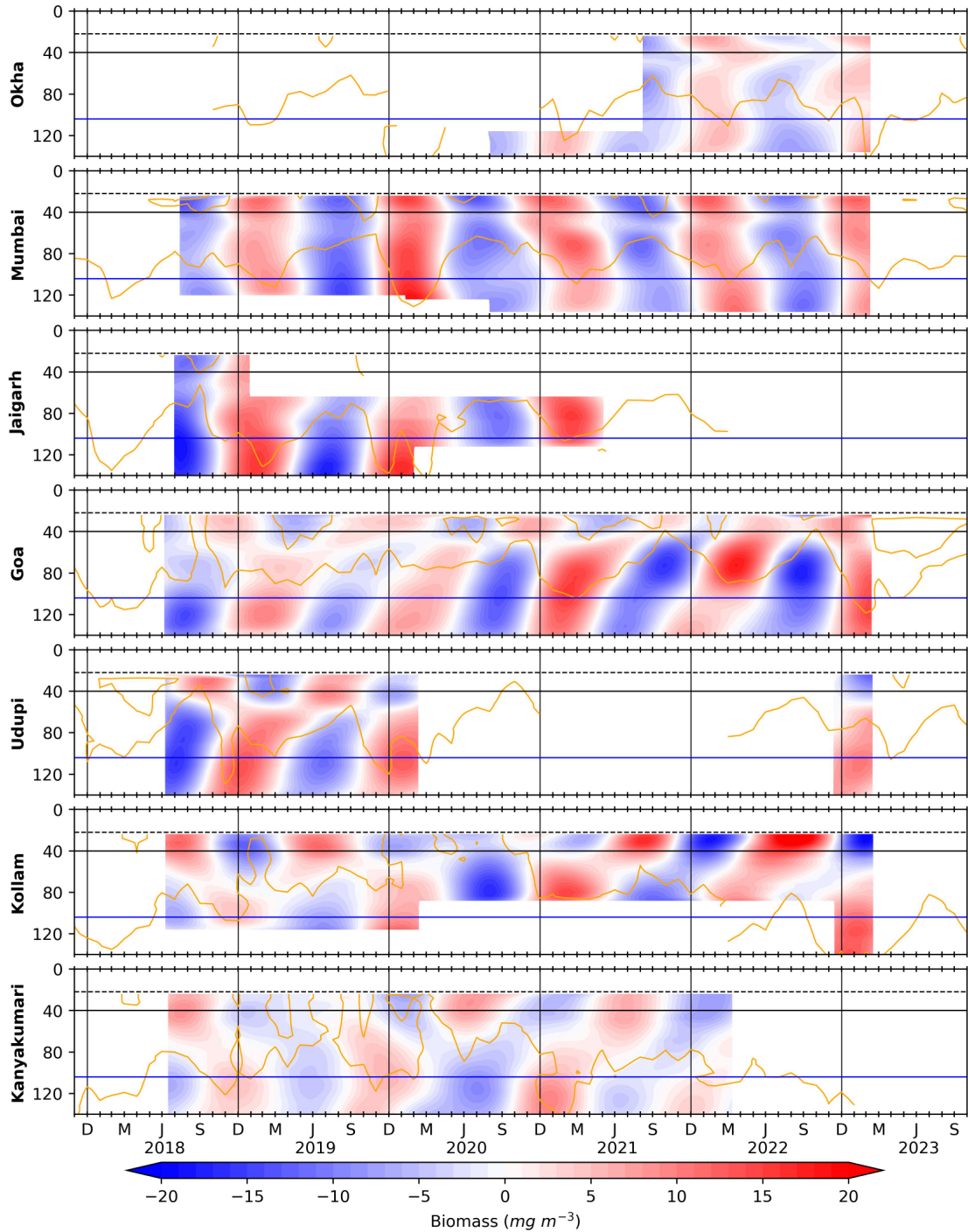


Figure 11: The biomass variation occurring in annual band (300 to 400 days). Owing to the presence of monsoon, there is a variation driven by associated upwelling (downwelling) processes in summer (winter) monsoon. and The horizontal black and blue lines is for 40 and 104 m respectively; vertical black lines separate the years. The dashed line at 22 m marks the top-depth of first bin i.e, 24 m and solid orange curves denotes D215 (D175 off Okha and Kanyakumari)

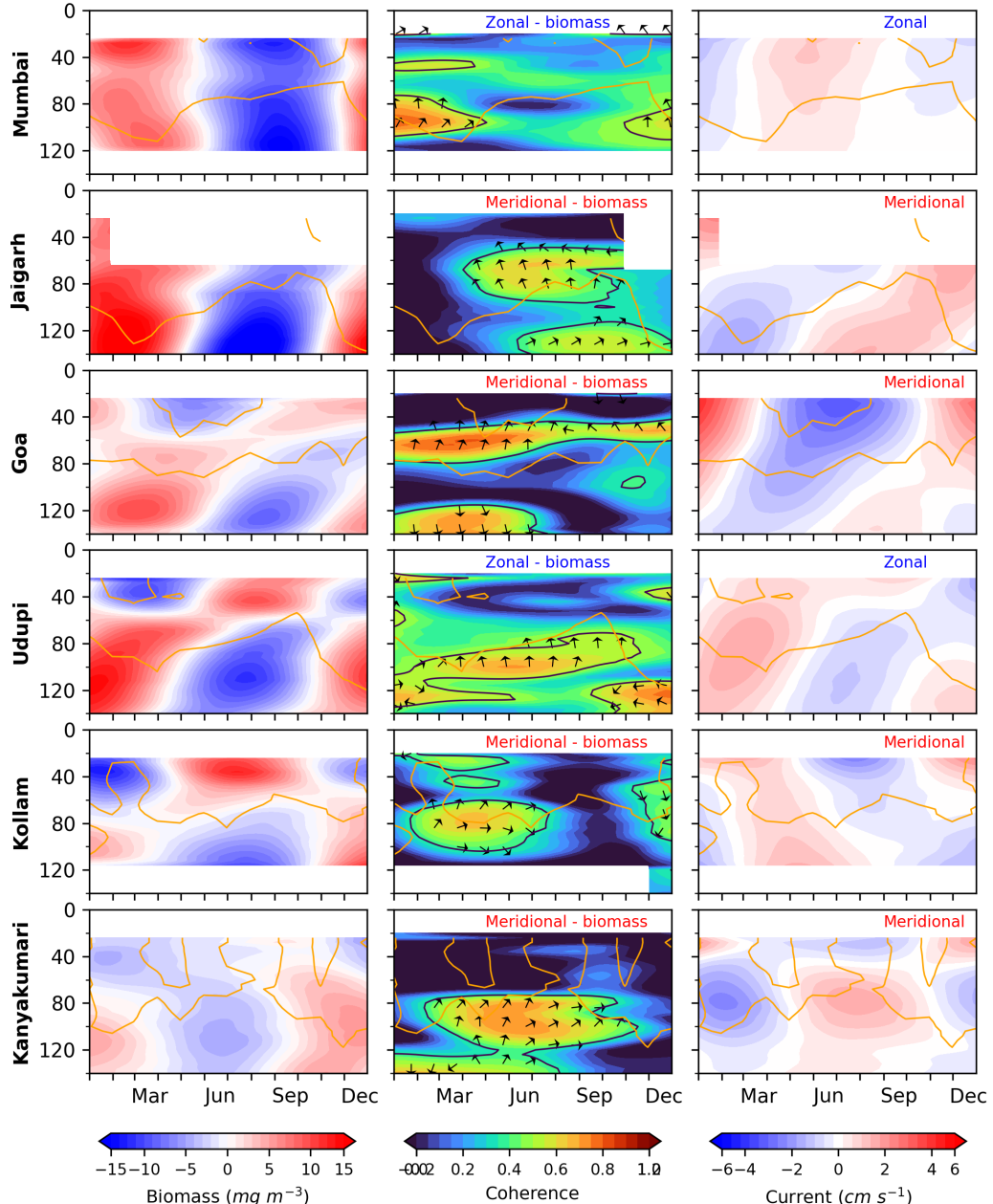


Figure 12: Current (zonal/meridional) and biomass wavelet coherence plotted alongside of annual filtered biomass and current. Either zonal or meridional current is considered depending on coherence and if current leads biomass. The solid contour encompasses greater than 0.5 coherence and phase is plotted with north as reference, +ve (-ve) x-axis is current leading (lagging) biomass. Left (Right) panel is for biomass (current). Although the annual biomass variability is weak and contributes less to the total biomass time series, upward phase propagation is seen implying upwelling favorable conditions leading to biomass growth. The solid orange curves denotes D215 (D175 off Okha and Kanyakumari)

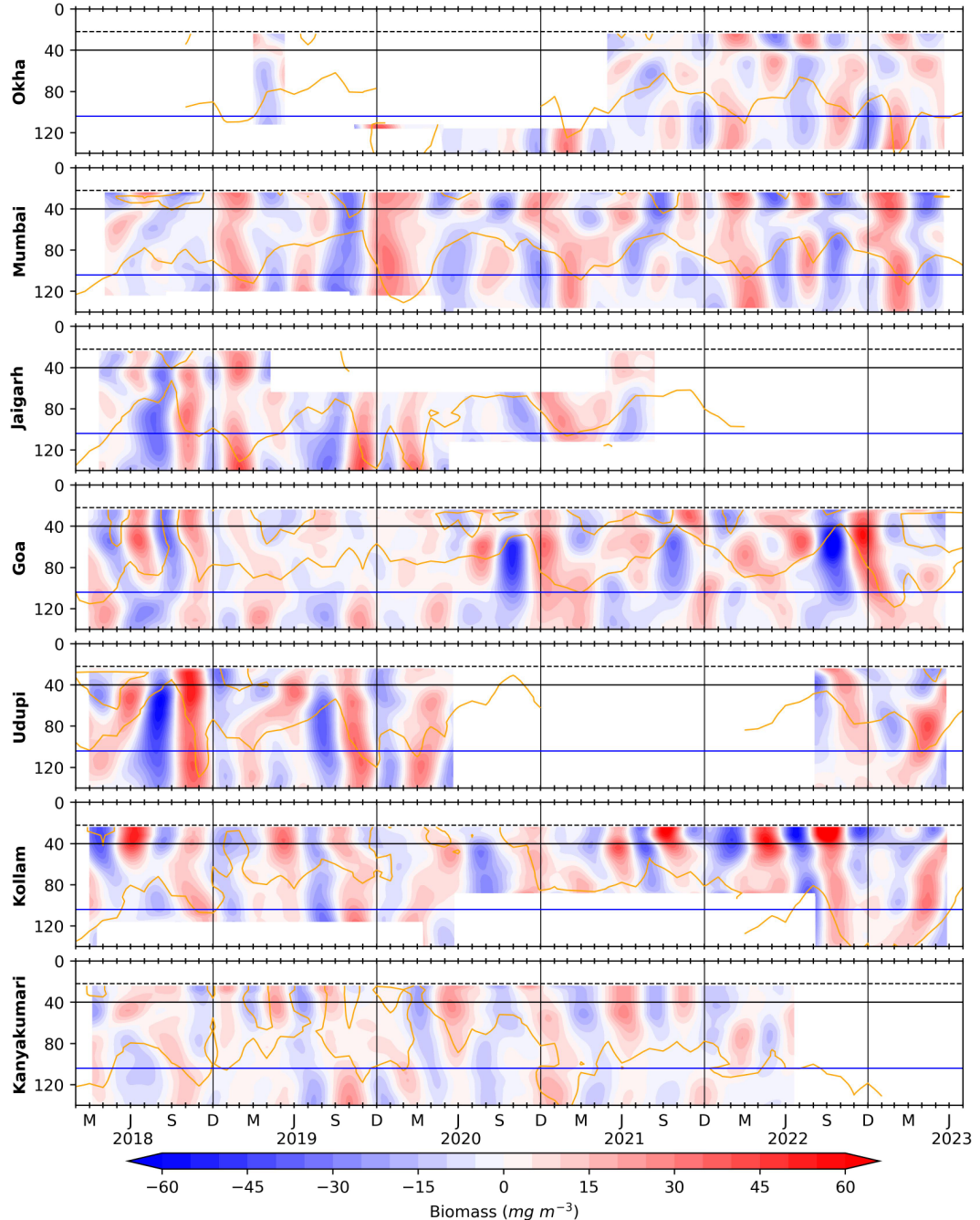


Figure 13: The biomass variation occurring in 100 to 250 days period (between the seasons and within a year record or intra-annual band) is obtained using a band pass filter. The horizontal black and blue lines is for 40 and 104 m respectively; vertical black lines separate the years. The dashed line at 22 m marks the top-depth of first bin i.e, 24 m and solid orange curves denotes D215 (D175 off Okha and Kanyakumari).

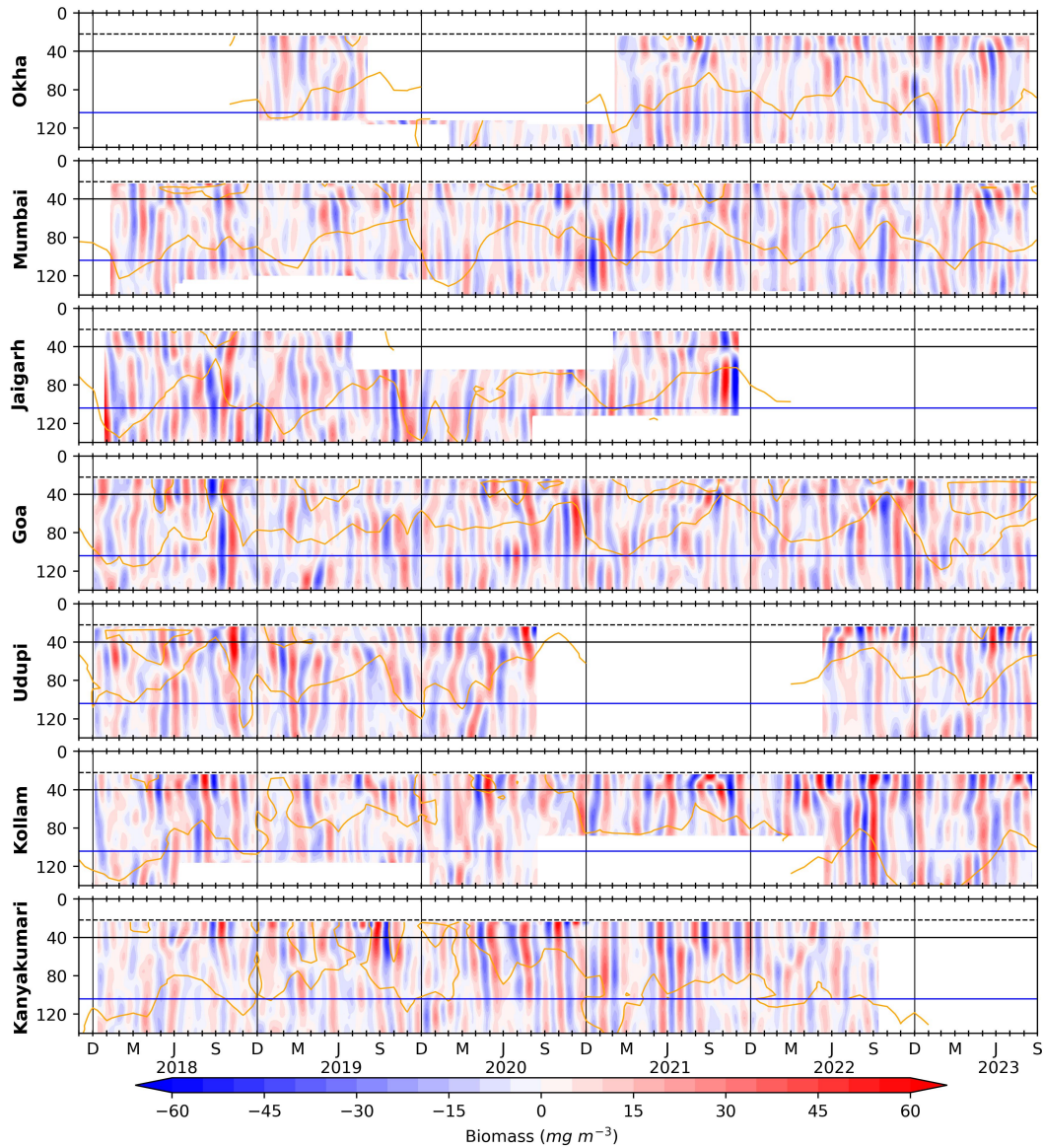


Figure 14: Biomass variation found in the scale of 30 to 90 days period (Intra-seasonal band as it is within a season) is obtained using a lanczos band pass filter. The horizontal black and blue lines is for 40 and 104 m respectively; vertical black lines separate the years. The dashed line at 22 m marks the top-depth of first bin i.e, 24 m. Intraseasonal variability is seen throughout the record and the variability is stronger during August to November.